ELSEVIER

Regular and stochastic behavior of Parkinsonian pathological tremor signals

R.M. Yulmetyev[a,b,*], S.A. Demin[a,b], O. Yu. Panischev[a,b], Peter Hänggi[c], S.F. Timashev[d], G.V. Vstovsky[e]

[a]*Department of Physics, Kazan State University, 420008 Kazan, Kremlevskaya Street, 18, Russian Federation*
[b]*Department of Physics, Kazan State Pedagogical University, 420021 Kazan, Mezhlauk Street, 1, Russian Federation*
[c]*Department of Physics, University of Augsburg, Universitätsstrasse 1, D-86135 Augsburg, Germany*
[d]*Karpov Institute of Physical Chemistry, 105064 Moskow, Vorontsovo Pole Street, 10, Russian Federation*
[e]*Semenov Institute of Chemical Physics, 117977 Moscow, Kosygina Street, 4, Russian Federation*

Abstract

Regular and stochastic behavior in the time series of Parkinsonian pathological tremor velocity is studied on the basis of the statistical theory of discrete non-Markov stochastic processes and flicker-noise spectroscopy. We have developed a new method of analyzing and diagnosing Parkinson's disease (PD) by taking into consideration discreteness, fluctuations, long- and short-range correlations, regular and stochastic behavior, Markov and non-Markov effects and dynamic alternation of relaxation modes in the initial time signals. The spectrum of the statistical non-Markovity parameter reflects Markovity and non-Markovity in the initial time series of tremor. The relaxation and kinetic parameters used in the method allow us to estimate the relaxation scales of diverse scenarios of the time signals produced by the patient in various dynamic states. The local time behavior of the initial time correlation function and the first point of the non-Markovity parameter give detailed information about the variation of pathological tremor in the local regions of the time series. The obtained results can be used to find the most effective method of reducing or suppressing pathological tremor in each individual case of a PD patient. Generally, the method allows one to assess the efficacy of the medical treatment for a group of PD patients.
© 2006 Elsevier B.V. All rights reserved.

Keywords: Discrete non-Markov processes; Flicker-noise spectroscopy; Time-series analysis; Parkinson's disease; Complex systems

1. Introduction. Parkinson's disease

Recently, much effort has been made in searching new alternative methods of diagnosing, treating and preventing severe diseases of central nervous and locomotor systems. Among them, Parkinson's disease (PD) is one of the most serious illnesses. PD, was called so by the French neurologist Pierre Marie Charcot in the 19th century to honor Dr. James Parkinson, who first described the disease in 1817. Dr. Parkinson presented the account of the observation results made, about six patients in his book *An essay on the shaking palsy*.

*Corresponding author.

E-mail addresses: rmy@theory.kazan-spu.ru (R.M. Yulmetyev), sergey@theory.kazan-spu.ru (S.A. Demin).

The present paper deals with two physical methods used in combination to analyze, diagnose and treat PD. The possibilities of the methods are assessed and compared. The comparison allowed us to add extra information about the behavior of PD pathological tremor physical parameters.

The first method is based on the notions and concepts of the statistical theory of discrete non-Markov stochastic processes [1,2]. The method is connected with the studies of statistical non-Markov effects, long- and short-range statistical memory effects, regularity and stochastic behavior effects, and dynamic alternation of relaxation modes in the patient in various dynamic states. The study of non-Markov effects in complex systems in biology [3–6], physics [6–9], seismology [10,11], and medicine [2,12–14] is of special interest for correlation analysis. The scale of time fluctuations, long-range effects, discreteness of various processes and states, and the effects of dynamic alternation in the initial time series are important role in this respect. The discreteness of experimental data, statistical effects of long- and short-range memory and the constructive role of fluctuations and correlations can be used to obtain information about the properties and parameters of the system under study. Within this method, a set of quantitative and qualitative parameters allows one to determine typical distinctions between the natural and after treatment states of a patient, describes a detailed variation in patient's pathological tremor, and helps to choose the most effective treatment of separate patients and statistical groups.

The second method, flicker-noise spectroscopy (FNS), is a general phenomenological approach to the analysis of the behavior of complex nonlinear systems. It is designed to extract the information contained in chaotic signals of various natures: time series, spatial series, and complex power spectra produced by the systems. Within the FNS method, the series of various irregularities (spikes, jumps, discontinuities of derivatives of various orders) of the dynamic variables of a system at all levels of its temporal and spatial hierarchy are analyzed to extract the information that can help to predict the behavior of the system. The use of irregularities in the dynamic variables as the information basis or "colors" of the FNS methodology enables us not only to classify all the information contained in the chaotic series in the most general phenomenological form, but also to extract distinctively any desired portion of this information. The FNS method can be used to solve three types of problems: to determine the parameters, or patterns, characterizing the behavior or structural features of open complex (physical, chemical, natural) systems; to determine the precursors of the sharpest changes in the state of open dissipative systems of various natures using the prior information about the behavior of the systems; to determine the redistribution behavior of excitations in the distributed systems by analyzing dynamic correlations in chaotic signals measured simultaneously at different points.

PD is a progressing chronic brain disease manifesting itself in movement disorders. PD is caused by complex biochemical processes accompanied by the lack of the chemical substance dopamine. Dopamine acts as a transmitter of signals from one nervous cell to another. The lack of the neurotransmitter dopamine causes changes in the brain parts that control human motor functions.

The origin of PD is not clear. It is most frequently believed that this disease is caused by a combination of three factors: biological aging, heredity and exposure to some toxins. The major PD symptoms are hypokinesia, stiffness and tremor. New ideas and principles are required to solve the problems emerging in classical treatment methods. The diagnostics of the disease in the early stages is one of these problems. Only the joint efforts of experts from different science areas can bring a solution to this kind of problems. For example, the modern methods of biophysics, biochemistry and neurophysiology enabled us to make considerable progress in understanding PD reasons and developing the methods of its treatment.

Today, there are three methods of PD treatment: medicamentous therapy, neurologic surgery and electromagnetic stimulation of certain brain areas. To obtain a more reliable picture of PD evolution, it is necessary to use physical methods. In this case, statistical methods of analysis are of special importance. They are used to analyze experimental time series of various parameters of tremor in patient's limbs. As a rule, the experimental data are obtained by conventional biomechanical methods [15–17] such as recording of electric signals in leg muscles when the patient is walking [18] or by laser recording of physiological and pathological tremor in human hands [19–23].

A nonlinear dynamical model is used to analyze a variety of human gaits [24]. The stride-interval time series in normal human gait is characterized by slightly multifractal fluctuations. The fractal nature of the fluctuations becomes more pronounced under both the increase and decrease in the average gait [24].

Nonlinear time series analysis is applied in studying normal and pathological human walking [18]. The problems caused by age changes in a human gait [25–28], various movement disorders and locomotor system diseases [29,30] are studied by Hausdorff. A nonlinear signal, multimodal (independent) oscillations, and the periodic pattern of time records in hand tremor and muscle activity in a PD patient are studied in Ref. [23]. PD patients exhibit tremor, involuntary movements of the limbs. Typically the frequency spectrum of tremor has broad peaks at "harmonic" frequencies, much like that is seen in other physical processes. In general, this type of harmonic structure in the frequency domain may be due to two possible mechanisms: a nonlinear oscillation or a superposition of (multiple) independent modes of oscillation [23]. Various dynamical states of PD patients are also studied by means of the time series of pathological tremor in fingers [31–35].

At present special attention is attached to the problems of distinguishing and analyzing of the stochastic and regular components of experimental time series of biological systems. Thereto various methods of nonlinear physics and simulation by nonlinear oscillators [36–40], the methods of fractal analysis of time series [41–46], the methods of detrended fluctuation analysis [47,48] are used.

In Ref. [36] Babloyantz et al. presented a simple graphical method that unveils subtle correlations between short sequences of a chaotic time series. Similar events, even from noisy and nonstationary data, are clustered together and appear as well-defined patterns on a two-dimensional diagram and can be quantified. The general method is applied to the electrocardiogram of a patient with a malfunctioning pacemaker, the residence times of trajectories in the Lorenz attractor as well as the logistic map. In this paper the authors introduced a simple graphical method that projects the trajectories of chaotic attractors into various planes in a way mat unveils very subtle correlations between consecutive sequences of events. The merit of the method resides in the fact that these sequences may extend over more than ten events. The sequences with similar relationships but not the same absolute values may appear as well-defined structures in a two-dimensional diagram. The advantage of this mapping is that, although the sequences may take into account more than three consecutive events, the two-dimensional projections are extremely helpful visual aides for elucidation of some aspects of chaotic dynamics.

Goldbeter et al. studied various biological rhythms which regulate the vital activity of living systems and determine the control mechanisms of these rhythms. In Ref. [38] the periodic oscillations at all levels of biological organization, with periods ranging from a fraction of a second to years were observed. The authors of Ref. [39] examined the mechanisms of transitions from simple to complex oscillatory phenomena in metabolic and genetic networks. The mechanisms underlying such transitions are examined in models for a variety of rhythmic processes in several live systems. Ref. [40] is devoted to the study of circadian oscillations stochastic dynamics and the influences the gene expression exerts on it. Authors show the way robust circadian oscillations are produced from a "bar-code" pattern of gene expression.

Liebovitch et al. reveal the local features of dynamics of various biological systems by the methods of fractal analysis and various methods of nonlinear physics. In Ref. [41] the question was examined: the way the dynamics of neural networks of the Hopfield type depends on the updating scheme, temperature dependence, degree of locality of connections between elements and the number of memories. Further the results were applied to interpret some features of protein dynamics. In Refs. [42,43] authors studied the self-organizing and the synchronization of the trajectory of a coupled systems dynamics. In particular, in Ref. [42] the authors introduced a scheme of controlling the dynamics of deterministic systems by coupling it to the dynamics of other similar systems. The controlled systems synchronized their dynamics with the control signal in periodic as well as chaotic regimes. In Ref. [44] the processes of transition from persistent to antipersistent correlation was studied by means of fractal analysis methods of a time series: fractional Brownian motion, rescaled range analysis, variance analysis, zero-crossing analysis. The authors discussed several simple random walk models which produce such transitions (bounded correlated random walk, fractional Brownian motion with a long relaxation time), and therefore are candidates for the mechanisms that may be present in some biological systems. The authors have studied the way the pattern, seen in the experimental data of biological systems, persistent at short time intervals and antipersistent at long time intervals, could arise from dynamical systems. The comparison of Hurst coefficient, which was calculated on the basis of different fractal analysis methods, was carried out. The article [45] is devoted to the study of the cardiac rhythm abnormalities by means of estimation of the probability density function and Hurst rescaled range analysis. In paper [46] the authors examined the effects of fractal ion-channel activity in modifications of two classical neuronal models:

Fitzhugh-Nagumo and Hodgkin-Huxley. The authors came to the conclusion that fractal ion channel gating activity was sufficient to account for the fractal-rate firing behavior.

In this paper a qualitatively new methodology of extracting the information from the time series on the united basis of the theory of discrete non-Markov stochastic processes and the FNS for the case of PD is submitted. This methodology presents a simple graphic and relatively inexpensive method of analysis of various physiological and pathological patient's states. In particular, it allows to make a quantitative estimation of the quality of treatment and to define the most effective method of treatment in each individual case and for a group of patients. We determine the structure of the initial time signal, and also the information about the nonstationary effects or about the dynamic alternation by a set of quantitative physical characteristics. We give special attention to the analysis of correlations and fluctuations which determine the time evolution in live systems.

In particular, the signals of PD pathological tremor are physically interpreted to answer the following questions:

(i) How can the study of the stochastic behavior and regularity in tremor signals help in evaluating the state of a PD patient?

(ii) How do certain physical parameters related to Markov and non-Markov features, statistical memory effects and dynamic alternation of relaxation modes in the initial time signal change?

(iii) How do the low- and high-frequency components of the initial time signal respond to the changes of pathological tremor in the patient under treatment?

2. Basic concepts and definition of statistical theory of discrete non-Markov random processes

The theory of discrete non-Markov stochastic processes [1,2] is based on the finite-difference representation of the kinetic Zwanzig–Mori's [49–52] for condensed matters, which are well known in the statistical physics of nonequilibrium processes. The theory is also widely used in analyzing complex biological and social systems. Dynamic, kinetic and relaxation parameters provided by this theory contain detailed information on a wide range of parameters and properties of complex systems.

Let the behavior of PD pathological tremor velocity be described by a discrete time series x_j of variable X:

$$X = \{x(T), x(T+\tau), x(T+2\tau), \ldots, x(T+\tau N - \tau)\}. \tag{1}$$

Here T is the time at which the recording of the pathological tremor is started, $(N-1)\tau$ is the total time of signal recording, and τ is the discretization time. In the system under study the discretization time is $\tau = 10^{-2}$ s. To describe the dynamic parameters of pathological tremor (correlation dynamics), it is convenient to use a normalized time correlation function (TCF):

$$a(t) = \frac{1}{(N-m)\sigma^2} \sum_{j=0}^{N-1-m} \delta x_j \delta x_{j+m} = \frac{1}{(N-m)\sigma^2} \sum_{j=0}^{N-1-m} \delta x(T+j\tau)\delta x(T+(j+m)\tau),$$

$$t = m\tau, \quad 1 \leqslant m \leqslant N-1. \tag{2}$$

TCF depending on current $t = m\tau$ can be conveniently used to analyze dynamic properties of complex systems. TCF usage means that the developed method is true of complex systems, when correlation function exists. The mean value $\langle X \rangle$, fluctuations δx_j, absolute (σ^2) and relative (δ^2) dispersion for a set of random variables (Eq. (1)) can be easily found by

$$\langle X \rangle = \frac{1}{N} \sum_{j=0}^{N-1} x(T+j\tau),$$

$$x_j = x(T+j\tau), \quad \delta x_j = x_j - \langle X \rangle,$$

$$\sigma^2 = \frac{1}{N} \sum_{j=0}^{N-1} \delta x_j, \quad \delta^2 = \frac{\sigma^2}{\langle X \rangle^2}.$$

The function $a(t)$ satisfies the normalization and relaxation conditions of correlations: $\lim_{t\to 0} a(t) = 1$, $\lim_{t\to\infty} a(t) = 0$.

By using the Zwanzig–Mori's technique of projection operators [49–52] it is possible to receive an interconnected chain of finite-difference equations of a non-Markovian type [1,2] for the initial TCF $a(t)$ and the normalized memory functions in the following way:

$$\frac{\Delta a(t)}{\Delta t} = \lambda_1 a(t) - \tau \Lambda_1 \sum_{j=0}^{m-1} M_1(j\tau) a(t - j\tau). \tag{3}$$

Here λ_1 is the eigenvalue and Λ_1 is the relaxation parameter of Liouville's quasioperator $\hat{L}$. Function $M_1(j\tau)$ is a normalized memory function of the first order:

$$\lambda_1 = i\frac{\langle \mathbf{A}_k^0(0)\hat{L}\mathbf{A}_k^0(0)\rangle}{\langle |\mathbf{A}_k^0(0)|^2\rangle}, \quad \Lambda_1 = \frac{\langle \mathbf{A}_k^0(0)\hat{L}_{12}\hat{L}_{21}\mathbf{A}_k^0(0)\rangle}{\langle |\mathbf{A}_k^0(0)|^2\rangle},$$

$$M_1(j\tau) = \frac{\langle \mathbf{A}_k^0(0)\hat{L}_{12}(1 + i\tau\hat{L}_{22})^j \mathbf{A}_k^0(0)\rangle}{\langle \mathbf{A}_k^0(0)\hat{L}_{12}\hat{L}_{21}\mathbf{A}_k^0(0)\rangle}, \quad M_1(0) = 1. \tag{4}$$

Gram–Schmidt orthogonalization procedure $\langle \mathbf{W}_n, \mathbf{W}_m\rangle = \delta_{n,m}\langle |\mathbf{W}_n|^2\rangle$, where $\delta_{n,m}$ is Kronecker's symbol, can be used to rewrite the above equations in a compact form:

$$\mathbf{W}_0 = \mathbf{A}_k^0(0), \quad \mathbf{W}_1 = (i\hat{L} - \lambda_1)\mathbf{W}_0, \quad \mathbf{W}_2 = (i\hat{L} - \lambda_2)\mathbf{W}_1 - \Lambda_1\mathbf{W}_0, \ldots,$$

$$\mathbf{W}_n = (i\hat{L} - \lambda_n)\mathbf{W}_{n-1} - \Lambda_{n-1}\mathbf{W}_{n-2} - \ldots.$$

Then the eigenvalue λ_1 of Liouville's quasioperator and the relaxation parameter Λ_1 in Eq. (3) take the form of:

$$\lambda_1 = i\frac{\langle \mathbf{W}_0\hat{L}\mathbf{W}_0\rangle}{\langle |\mathbf{W}_0|^2\rangle}, \quad \Lambda_1 = i\frac{\langle \mathbf{W}_0\hat{L}\mathbf{W}_1\rangle}{\langle |\mathbf{W}_0|^2\rangle}.$$

The normalized memory function of the first order in Eq. (3) is rewritten as

$$M_1(t) = \frac{\langle \mathbf{W}_1(1 + i\tau\hat{L}_{22})^m\mathbf{W}_1\rangle}{\langle |\mathbf{W}_1(0)|^2\rangle}.$$

The finite-difference kinetic (3) represents the generalization of Zwanzig–Mori's kinetic theory [49–52], which is well known in statistical physics, for complex discrete non-Hamiltonian statistical systems. Within our method of the analysis of dynamics of the statistical time series we do not use Eq. (3) as an object for the subsequent theoretical analysis. In this connection we do not use the equations such as Zwanzig–Mori's for memory functions of the second and higher orders. We use the algorithm, which was above described, to calculate the time dynamics $a(t)$, $M_1(t)$ and parameters λ_1, Λ_1. The dependences $a(t)$ and $M_1(t)$ are calculated on the basis of the experimental data, independently of each other. At the same time we control the conformity of the calculated dependences $a(t)$, $M_1(t)$ and parameters λ_1, Λ_1 to Eq. (3) (the precision of the conformity is $\sim$2–5% for the cases described here). We use the dependences $a(t)$ and $M_1(t)$ to analyze the amplitude of Parkinsonian tremor velocity. We also use these dependences to calculate the non-Markovity parameter [1,2] which characterizes the degree of correlativity of the signal. The studies, which have been carried out earlier [2,12,13], show that this parameter contains detailed information about the physiological state of a system.

In this paper, we shall use the spectral dependence $\varepsilon_1(v)$ of the first point of the non-Markovity parameter [1,2]:

$$\varepsilon_1(v) = \left\{\frac{\mu_0(v)}{\mu_1(v)}\right\}^{1/2}, \tag{5}$$

which is determined by means of Fourier transformations $\mu_0(v)$, $\mu_1(v)$ of functions $a(t)$ and $M_1(t)$, respectively:

$$\mu_0(v) = \left| \sum_{j=0}^{N-1} a(t_j) \cos(2\pi v t_j) \right|^2, \quad \mu_1(v) = \left| \sum_{j=0}^{N-1} M_1(t_j) \cos(2\pi v t_j) \right|^2.$$

Further we shall show, that the application of the frequency-dependence $\varepsilon_1(v)$ and the values of this parameter on zero frequency:

$$\varepsilon_1(v = 0) = \varepsilon_1(0) = \left\{ \frac{\mu_0(0)}{\mu_1(0)} \right\}^{1/2}, \tag{6}$$

allows to introduce the quantitative estimations for various dynamic states of a patient with PD. In particular, we shall show, that the values of parameter $\varepsilon_1(0) \sim 10^1$ for the analyzed system are characteristic of stable physiological states (for the patient under treatment). The appearance of pathology in a system leads to a sharp decrease in this parameter, approximately by one order. Thus, we can compare quantitatively various dynamic states of the studied system considering the changes of the non-Markovity parameter.

3. Flicker-noise spectroscopy for analysis of time series of dynamic variables

New information about chaotic time signals can be obtained by the method of the FNS [53–57]. Its advantage consists in extracting information from the series of distinct irregularities (spikes, jumps, discontinuities of derivatives of various orders) by analyzing the behavior of time, spatial and power dynamic variables at each existential level of the hierarchical organization of the system. Thus, the most valuable information is obtained by analyzing the power spectra and the difference moments ("structural functions") of various orders. It is necessary to point out, that the difference moments are formed exclusively by irregularities of a jump type. On the other hand, the power spectra are formed by the contributions of two types of irregularities: peaks and jumps.

The FNS method was applied to analyze the dynamics of various physical and chemical processes [58–65]. Among them are fluctuations of electric voltage in electrochemical systems (considered in the process of formation of porous silicon under conditions of anodic polarization, formation of molecular hydrogen on platinum under cathodic polarization, initiation of hydrodynamical instability in the field of an over-limiting current in electro-membrane systems), fluctuating dynamics of the solar activity, fluctuation of a velocity component in turbulent streams. Unique abilities of the FNS method to locate the multipoint correlation interrelations were shown in Refs. [66–68]. That was done on the basis of the analysis of simultaneously measured signals at spaced points of the distributed systems.

The basic relations of FNS are given below. We analyze the chaotic series of dynamic variable $x(t)$ over the time interval $T_{tot} = N\tau$, where τ is a sampling time.

1. We proceed from the notion of hierarchy of spatial-temporal levels of the organization of open dynamic dissipative systems.

2. The most valuable information in the chaotic series is stored in irregularities of various types, such as peaks, jumps, breaks of derivatives of different orders. The parameters which characterize the properties of irregularities, can be obtained by the analysis of power spectra $S(f)$ (f is a frequency):

$$S(f) = \left[\frac{1}{N} \sum_{k=1}^{N} \delta x_k \cos(2\pi f k \tau) \right]^2 + \left[\frac{1}{N} \sum_{k=1}^{N} \delta x_k \sin(2\pi f k \tau) \right]^2, \tag{7}$$

where $x_k = x(T + t_k)$ and $t_k = k\tau$,

$$\delta x_k = x_k - \frac{1}{N} \sum_{k=1}^{N} x_k$$

and also by the analysis of transitive difference moments ("transitive structural functions") $\Phi^{(2)}(t_n)$ of the second order:

$$\Phi^{(2)}(t_n) = \frac{1}{N-n} \sum_{k=1}^{N-n} [x(t_k) - x(t_{k+n})]^2, \tag{8}$$

where t_n is a delay parameter. Further, when considering the dependence $\Phi^{(2)}(t_n)$ we will not specify the bottom index.

It should be noted that the proposed averaging procedure differs from Gibbs's procedure when averaging is carried out by using the probability density. Actually, we do not consider the statistics of ensembles as it is done in the statistical Gibbs's thermodynamics which is based on ergodic hypothesis. We also generalize Einstein's approach to the analysis of fluctuation dynamics [69,70].

3. Parameters or "passport data", obtained by the analysis of dependences $S(f)$ and $\Phi^{(2)}(t_n)$, are correlation times and dimensionless parameters. These dimensionless parameters describe the loss of "memory" (correlation relations) in irregularities of a "spikes" and "jumps" type.

4. For stationary processes in open dissipative systems the moment $\Phi^{(2)}(t_n)$ depends only on the difference of arguments $n\tau$. The self-similar structure is realized in this case. It means that the dependences $S(f)$ or $\Phi^{(2)}(t_n)$ are identical for each level of the system hierarchy.

It should be noted, that the reverse transformations in the FNS methodology are not used in the way it takes place in Fourier- or in wavelet-analysis. Therefore, no constraints are imposed on the character of the dependence $x(t)$ except for the existence of average values.

3.1. Basic equations for stationary processes

Let us obtain approximations for $S(f)$ and $\Phi^{(2)}(t_n)$, which are determined by irregularities in the behavior of dynamic variables. At the first stage the generalized δ-functions are used to approximate the spikes of the dynamic variables, and Heavyside functions are used to approximate the jumps. At the same time the "low-frequency" limit $f \ll 1/2\pi T_i$ is considered, when the characteristic time intervals T_i between the nearest irregularities are much less than all the characteristic times of the considered system. In case of stationary processes the obtained expressions are the same for each of the hierarchical levels. Then simple approximation dependence (see Refs. [53–57] for more information) can be obtained for $S(f)$ and $\Phi^{(2)}(t_n)$.

The approximation for the structural function of the second order reads:

$$\Phi^{(2)}(t) = 2 \cdot \sigma^2 \cdot [1 - \Gamma^{-1}(H_1) \cdot \Gamma(H_1, t/T_1)]^2. \tag{9}$$

Here $\Gamma(s)$ and $\Gamma(s, x)$ are, respectively, the gamma-function and incomplete gamma-function ($x \geqslant 0$ and $s > 0$); σ is dispersion of the measured dynamic variable with dimension $[x]$. Value H_1 is a Hurst's parameter. It characterizes the rate of loss of "memory" during the time intervals shorter than the correlation time T_1. As follows from Eq. (9), $\Phi^{(2)}(t) \to \sigma^2$ for $t \gg T_1$, parameter T_1 actually characterizes the time interval during which "forgetting" of the previous value of the dynamic variable occurs. Such "forgetting" is the consequence of the "jumps" of the dynamic variable at each level of the spatio-temporal hierarchy. True, the structural function is zero, $\Phi^{(2)}(t) = 0$, for the sequences of the irregularities-spikes, which are represented by a sequence of δ-functions (see Chapter 4.3 (Fig. 51) of Schuster's monograph [70]). At the same time, a continuous power spectrum $S(f)$ can be calculated for the correlated sequence of δ-functions within a low-frequency limit at $f \ll 1/2\pi T_i$, as was shown in Ref. [70]. $S(f)$ is determined by a correlation character of the analyzed sequence of the generalized functions. In particular, $S(f)$ can have dependence of a flicker-noise type: $S(f) \sim 1/f^s$, where $s \sim 1$. The conclusion about diverse information carried by the power spectra and the difference moments underlies the FNS method. Some artificial time series, generalizing the image of the signal as the sequence of δ-functions, earlier introduced by Schuster is used in this case.

Any signal, formed exclusively by irregularities-jumps, can be subject to Fourier transformation to obtain the power spectrum. Thus, the difference moment $\Phi^{(2)}(t)$ is formed only by jumps of a dynamic variable at different spatio-temporal levels of the system hierarchy, and both spikes and jumps contribute to the power spectrum $S(f)$.

The standard notion about the identity of the information represented by $\Phi^{(2)}(t)$ and $S(f)$, is valid only for "smooth" functions. However, real signals $V(t)$ are never smooth. Therefore, the FNS method focuses on giving the essence of information on sequences of irregularities latent in real signals and eliminates information discrepancy, making it possible to extract the information by considering various features.

Eq. (9) can be used to find the phenomenological parameters $[H_1, T_1, \sigma]$. Contribution $S_J(f)$ to the power spectrum $S(f)$, determined by the influence of irregularities, such as jumps, is expressed by the formula:

$$S_J(f) \approx S_J(0) \frac{1}{1 + (2\pi T_1 f)^{2H_1+1}}, \tag{10}$$

$$S_J(0) = 4\sigma^2 T_1 H_1 \left\{ 1 - \frac{1}{2H_1 \Gamma^2(H_1)} \int_0^\infty \Gamma^2(H_1, \xi)\, d\xi \right\}.$$

Due to spikes the contribution $S_B(f)$ to power spectrum $S(f)$ can be generally presented as the expression:

$$S_B(f) \approx \frac{S_B(0)}{1 + (2\pi f T_{00})^{n_0}}, \tag{11}$$

where parameter n_0 characterizes the velocity of the "losses of memory" (correlation relations) in a sequence of spikes during the time intervals shorter than the correlation time T_{00}. Parameters $[n_0, T_{00}, S_B(0)]$ characterize self-similarity in the correlation relations of the peaks. For the resulting power spectrum an approximation is used:

$$S(f) \approx \frac{S(0)}{1 + (2\pi f T_0)^n}, \tag{12}$$

where $S(0)$, T_0 and n are phenomenological parameters. The parameters which are determined in such a way differ from the parameters which are used in Eq. (10): $S_J(0) \neq S_B(0)$, $T_1 \neq T_0$ and $2H_1 + 1 \neq n_0$. So, the parameters determined from the power spectra and the structural functions of the second order give different information. The comparison of the parameters obtained by the analysis of the experimental series with numerical values of the parameters for model cases (Fick diffusion, Levy diffusion, Kolmogorov turbulence, turbulent diffusion, see Ref. [57]) allows to estimate qualitatively the character of the studied evolution (see Ref. [57] for more information).

The use of irregularities such as spikes, jumps, discontinuities of derivatives as the information basis of the FNS method allows to classify and extract phenomenological information contained in chaotic series. However, evolution of real biological systems has a more complex and nonstationary nature. In particular, the resonance frequencies in the dependences described above, can be specific for the studied system. The resonance frequencies appear as peaks in the power spectra $S(f)$ and the oscillatory character of function $\Phi^{(2)}(t)$. Thus, the values of resonance frequencies can change during the nonstationary evolution. Therefore for each state of the studied dynamics, the dependences $S(f)$ and $\Phi^{(2)}(t)$ are to be considered as "patterns" or "cliche". These dependences allow to estimate individual informational characteristics of the state of the system: times of loss of correlation relations, sets of specific frequencies, factors of nonstationarity. This will be demonstrated below in the analysis of Parkinsonian tremor dynamics.

3.2. Relaxation smoothing of signal, splitting into "low-frequency" and "high-frequency" components

In the analysis of the experimental series we frequently face the problem of smoothing of the initial signals. Usually the smoothing polynoms and wavelets are used to filtrate a signal and to extract a low-frequency component. Here we will describe briefly the method [57] of splitting the signal into "low-frequency" $x_R(t)$ and "high-frequency" $x_F(t)$ components. The method is based on an iterative procedure of a numeric solution of a heat conductivity equation:

$$\frac{\partial x}{\partial \tau} = \chi \frac{\partial^2 x}{\partial t^2}. \tag{13}$$

It uses an elementary explicit finite difference scheme:

$$\frac{x_k^{j+1} - x_k^j}{\Delta\tau} = \chi\frac{x_{k+1}^j + x_{k-1}^j - 2x_k^j}{(\Delta t)^2}, \tag{14}$$

that gives:

$$x_k^{j+1} = x_k^j + \frac{\chi\Delta\tau}{(\Delta t)^2}(x_{k+1}^j + x_{k-1}^j - 2x_k^j). \tag{15a}$$

Using designation $D = \chi\Delta\tau/(\Delta t)^2$, where D is a diffusion coefficient, we shall rewrite the last equation as

$$x_k^{j+1} = Dx_{k+1}^j + Dx_{k-1}^j + (1 - 2D)x_k^j. \tag{15b}$$

Iterations of this formula give a stable solution to $D < \frac{1}{2}$ [57]. For the smoothing procedure it is necessary to set limiting conditions. Let smoothing be carried out for a series of M samples (points). At each step of iterations extreme values for $k = 1$ and M are calculated as

$$x_1^{j+1} = (1 - 2D)x_1^j + 2Dx_2^j, \quad x_M^{j+1} = (1 - 2D)x_m^j + 2Dx_{M-1}^j. \tag{15c}$$

When calculating new values of signal x_k^{j+1} for $j + 1$ "relaxation" step by the values x_k^j (for $j = 0$ the initial signal $x(t)$ is set) we can obtain "low-frequency" component x_R. "High-frequency" component x_F is obtained by subtracting it from the initial signal. Actually, the smoothing procedure corresponds to the consecutive reduction of local gradients of values of variables with mutual rapprochement of points. The splitting of the initial signal $x(t)$ into two components $x_R(t)$ and $x_F(t)$ enables us to calculate the dependences $S(f)$ and $\Phi^{(2)}(t)$ for three functions $x_J(t)$ ($J = R, F$ or $G = R + F$). Index G is used for the initial signal $x(t)$. In particular, the low-frequency ("flicker-noise") component, which is present in any chaotic signal, is effectively removed when calculating dependence $S_F(f)$. Therefore, specific frequencies of the studied system come to light. This will be shown below in the analysis of the fluctuations of Parkinsonian tremor velocity. The analysis of dependences $S(f)$ and $\Phi^{(2)}(t)$, which are calculated separately for each of components R and F, presents special interest for the study of medical parameters.

4. Analysis of experimental data. Velocity of pathological tremor in patients with Parkinson's disease

As the experimental data we use the time records of pathological tremor velocity in an index finger of patients with PD [71,72].

Sixteen subjects with PD participated in the study. All subjects were receiving chronic stimulation either uni- or bilaterally to relieve the symptoms of PD including tremor, dyskinesia or rigidity. The participants received deep brain stimulation (DBS) of the internal globus pallidus (GPi) or subthalamic nucleus (STN), or ventrointermediate nucleus of the thalamus (Vim). They were all under 70 years of age and the group included 11 males and five females. All participants were clinically stable at the moment of the tests; they did not show cognitive impairment and did not suffer from a major depressive disorder. All subjects were under minimum dopaminergic therapy (ranging from 300 to 1200 mg per day of L-Dopa) at the time of the study and took other PD related medications.

The selected subjects were asked to refrain from taking their medication for at least 12 h before the beginning of the tests and were allowed to have not more than one coffee for breakfast on the two testing days. Rest tremor was recorded on the most affected side with a velocity-transducing laser [73,74]. This laser is a safe (Class II) helium–neon laser. The laser beam is split, with one part directed at the finger and the other, called the reference, directed at a rotating disk inside the laser. Back scattered light from the rotating disk is used to determine the sign of the velocity signal. Finger tremor was detected and converted into a calibrated voltage output proportional to finger velocity. Velocity is more sensitive to low-frequency components inherent in pathological and physiological tremor [74]. Than acceleration is the system did not require any special calibration procedure. The laser was placed at about 30 cm from the index finger tip and the laser beam was directed perpendicular to a piece of a reflective tape placed on the finger tip.

Tremor was recorded with a velocity laser under two conditions of DBS (on–off), under two conditions of medication (L-Dopa on–off) and under four conditions of 15, 30, 45, 60 min periods after stopping DBS. The conditions, counterbalanced among the subjects included the following.

1. The "OFF–OFF" condition (no medication and no stimulation).
2. The "ON–ON" condition (on medication and on stimulation).
3. The DBS condition—the "ON–OFF" condition (stimulation only).
4. The L-Dopa condition—the "OFF–ON" condition (no stimulation).
5–8. The "15 OFF", "30 OFF", "45 OFF", "60 OFF" conditions—the patient's states 15, 30, 45, 60 min after the DBS is switched off, no medication.

5. Discussion of results. Comparison of statistical theory of discrete non-Markov random processes and Flicker-noise spectroscopy

In this section we present the results of the analysis of the experimental data [71–73], which are obtained on the basis of the statistical theory of discrete non-Markov stochastic processes and the FNS. As an demonstrative example, we describe the results for one of the patients (the sixth patient, a woman, 61 years-old, deep brain stimulated bilaterally target structures: subthalamic nucleus, total daily medication 300 mg). The analysis the of experimental data allows to reveal some dynamic properties of PD tremor in each individual case and a group of patients. The obtained results characterize the group of 16 patients in a general way.

5.1. Non-Markovity, randomness, dynamic alternation and pathological tremor caused by Parkinson's disease

In Fig. 1 the initial time series of Parkinsonian tremor velocity of the patient's (sixth patient) index finger tremor is shown. By this record it is possible to reveal great differences (see the vertical scale) in tremor velocity of the patient's state, when the treatment is not used (Fig. 1a) and under medical treatment (Figs. 1b–d). The amplitudes of the tremor velocity for the "OFF–OFF" patient's state (Fig. 1a) and for the "ON–ON" state (Fig. 1b) differ by 94 times on average. The amplitude of tremor velocity when the DBS is switched off ("15 OFF", "30 OFF", "45 OFF", "60 OFF" conditions) (Figs. 1e–h) has a residual periodic character. The analysis of the initial time records does not allow to determine a method with the best medical effect. In some cases (Figs. 1e, h) a medical method produces a negative effect that results in the amplitude increase of tremor velocity and deterioration of the state of the patient. It is difficult to draw a conclusion about the efficacy of this or that treatment and to explain the after effect of the DBS based on the initial time signals.

A different representation of the signal allows to reveal the effects of periodicity and randomness in the initial time series. In Fig. 2 the initial time series of tremor velocity in two states of the patient (see Figs. 1a, d) are shown. We have chosen some local areas (500 points) of these time records. For the "OFF–OFF" patient's state (Fig. 2c) the initial time signal has a periodic structure. Similar periodicity of the initial time signal is connected to pathological tremor of the patient's limbs (with frequency $v = 5.2$ Hz). Retention of the structure is also observed when the DBS is switched off (see Figs. 1e–h). Medication produces a different effect on the patient ("OFF–ON" state, see Fig. 2d). The periodicity of the initial signal is replaced by randomness. The similar picture is characteristic of all methods of treatment (see Figs. 1b–d). This conclusion confirms the general idea about the transition of stochastic dynamic modes in case of the patient's normal physiological state to the periodic modes in a pathological state. This reasoning was confirmed by the analysis of the initial time series of all 16 patients.

The plane projections of phase trajectories of the two first dynamic orthogonal variables W_0, W_1 (see Section 2) in various states of the patient are shown in Fig. 3. All figures are submitted according to the initial time series. The structure of the phase trajectories is determined by the presence of fluctuations in the initial time series. The most significant fluctuations lead to deformation of phase clouds. The phase portraits consist of empty cores and helicoidal trajectories with a high concentration of phase points in the "OFF–OFF"
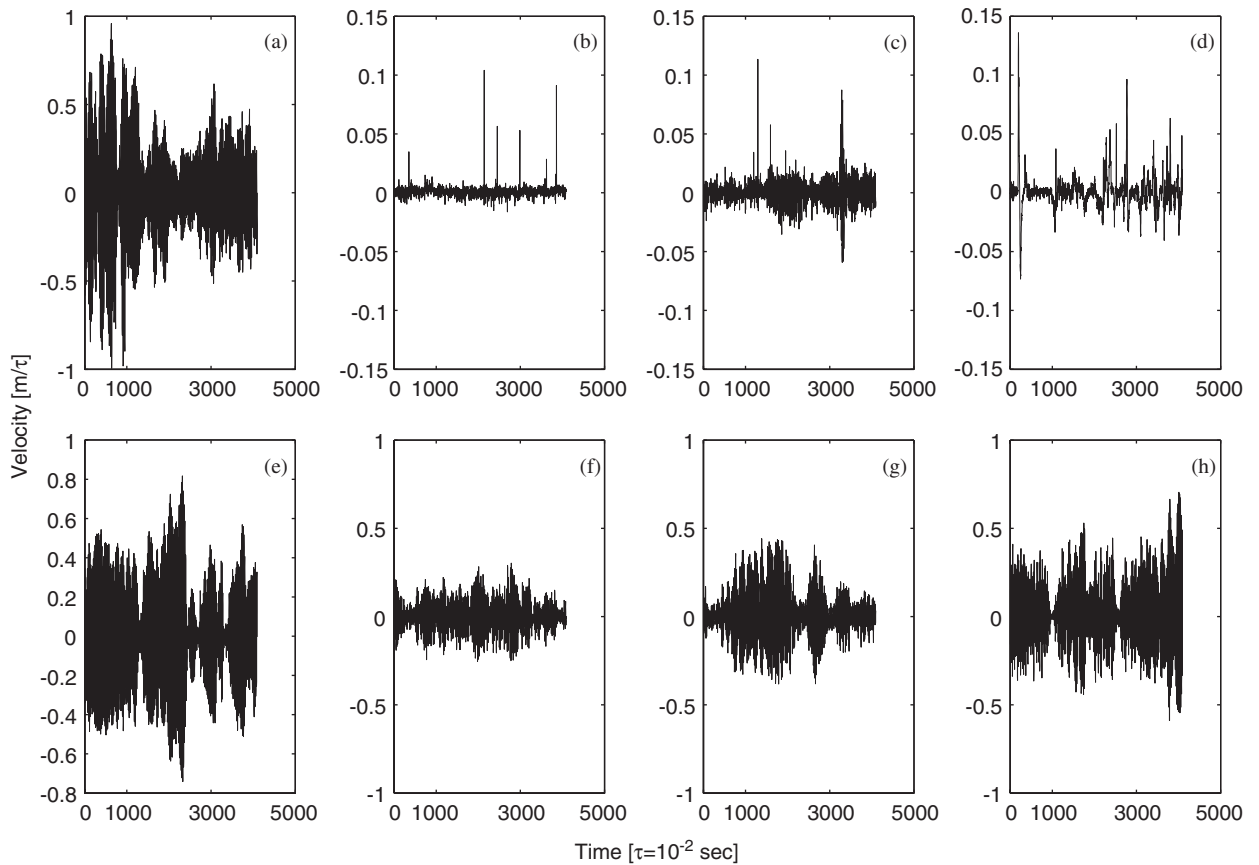
Fig. 1. Pathological tremor velocity in the left index finger of the sixth patient with Parkinson's disease. The registration of Parkinsonian tremor velocity is carried out in the following conditions: (a) "OFF–OFF" condition (no treatment); (b) "ON–ON" condition (using DBS and medicaments); (c) "ON–OFF" condition (DBS only); (d) "OFF–ON" condition (medicaments (L-Dopa) only); (e)–(h) the "15 OFF", "30 OFF", "45 OFF", "60 OFF" conditions—the patient's states 15 (30, 45, 60) min after the DBS is switched off, no treatment. Let us note the scale of the pathological tremor amplitude (see the vertical scale). Such representation of the time series allows us to note the increase or the decrease of pathological tremor.

patient's state (Fig. 3a) and in the cases when the DBS is switched off ("15 OFF", "30 OFF", "45 OFF", "60 OFF", see Figs. 3e–h). The presence of empty cores is explained by the insignificant quantity of small fluctuations near a zero value. Such structure of the phase portrait is determined by periodicity in the initial time signal (Fig. 2c). Here one can note a completely different picture of the effect any medical treatment has on the patient's organism. One can see rare significant fluctuations instead of small fluctuations of tremor velocity. These peak deviations result in acute-angled deformations of the central cores with a high concentration of phase points. The form of phase portraits corresponds to the dynamic alternation of periodic and stochastic components of the initial time signal. It is possible to draw a conclusion about the most effective method of treatment of each patient judging by the form of phase clouds. For the sixth patient two methods of treatment are almost equivalent: the complex treatment of a patient by two medical methods (Fig. 3b) and by using medicaments only (Fig. 3d).

The initial TCF power spectrum $\mu_0(v)$ (see Section 2) in various physiological states of the patient is shown in Fig. 4. All dependences are presented on a log–log scale. At characteristic frequency $v = 5.2$ Hz the peak is observed for each power spectrum. The peak amplitude is determined by the amplitude of tremor velocity in the initial time signal. In case of any medical treatment the peak amplitude considerably decreases. It happens because the amplitude of pathological tremor decreases. Any power spectrum reflects dynamic alternation effects in the initial time series. Oscillations are seen in the power spectra (Figs. 4a, e–h). Their periodic nature
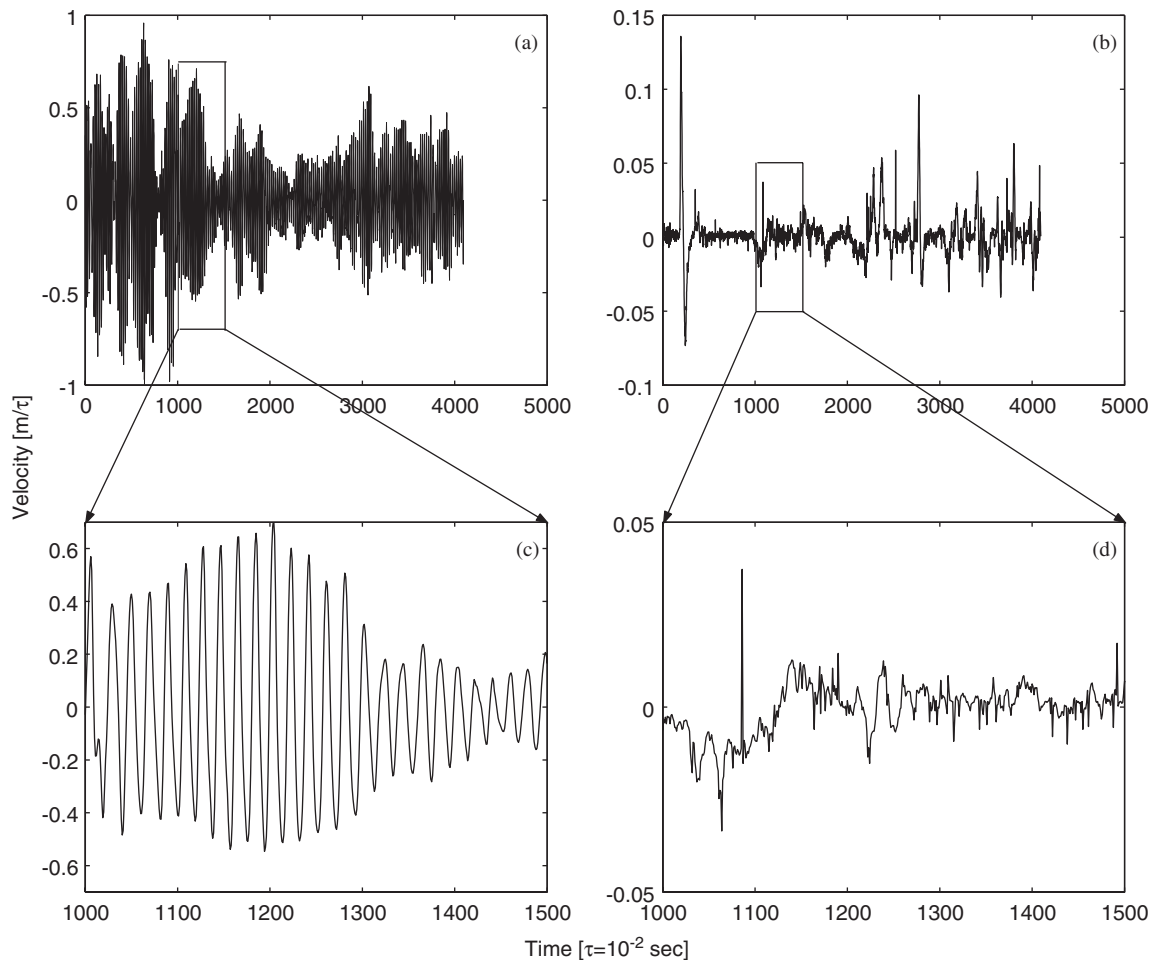
Fig. 2. The examples of the time series of some areas of pathological tremor velocity in the sixth patient: (a) The patient's state with no treatment. (b) The patient with treatment (medicaments only). The length of local sites of the time series constitutes 500 points. The local representation clearly reflects the structure of the initial time signal. (c) The regularity and the periodic nature of pathological tremor in the patient's state with no treatment. (d) The randomness of the tremor time signal of the patient under medicamentous treatment.

is clearly expressed by a low-frequency range. The periodic structure of the power spectra is broken, oscillations disappear, the amplitude of the peak on frequency $v = 5.2$ Hz decreases under treatment. Such form of the power spectra is connected to the amplification of randomness effects in the initial time series. The periodic nature of the patient's Parkinsonian tremor velocity is replaced by stochastic fluctuations with a low amplitude of tremor velocity. On the whole, the comparative analysis of the power spectra shows that medicamentous treatment has the most significant effect on the patient's organism (thus the combined use of medicaments and DBS is almost equivalent). The use of DBS stimulation does not decrease abnormal oscillations significantly.

The effects of randomness and regularity are most visible in the frequency dependences of the first point of the non-Markov parameter $\varepsilon_1(v)$. The physical idea of this parameter consists in revelation of Markov and non-Markov features in the time series. This parameter classifies all stochastic processes into random Markov processes $\varepsilon \gg 1$, quasi-Markov (intermediate) processes $\varepsilon > 1$ and non-Markov processes $\varepsilon \sim 1$. Thus, the first point of the non-Markovity parameter at zero frequency $\varepsilon_1(0)$ contains the most significant information. This point accumulates the information about all dynamic peculiarities of the time series. The increase of this value testifies to the amplification of Markov random effects in the time signals and the appearance of the effects of short range or instant memory. Thus, the comparative analysis of various physiological states of the patient
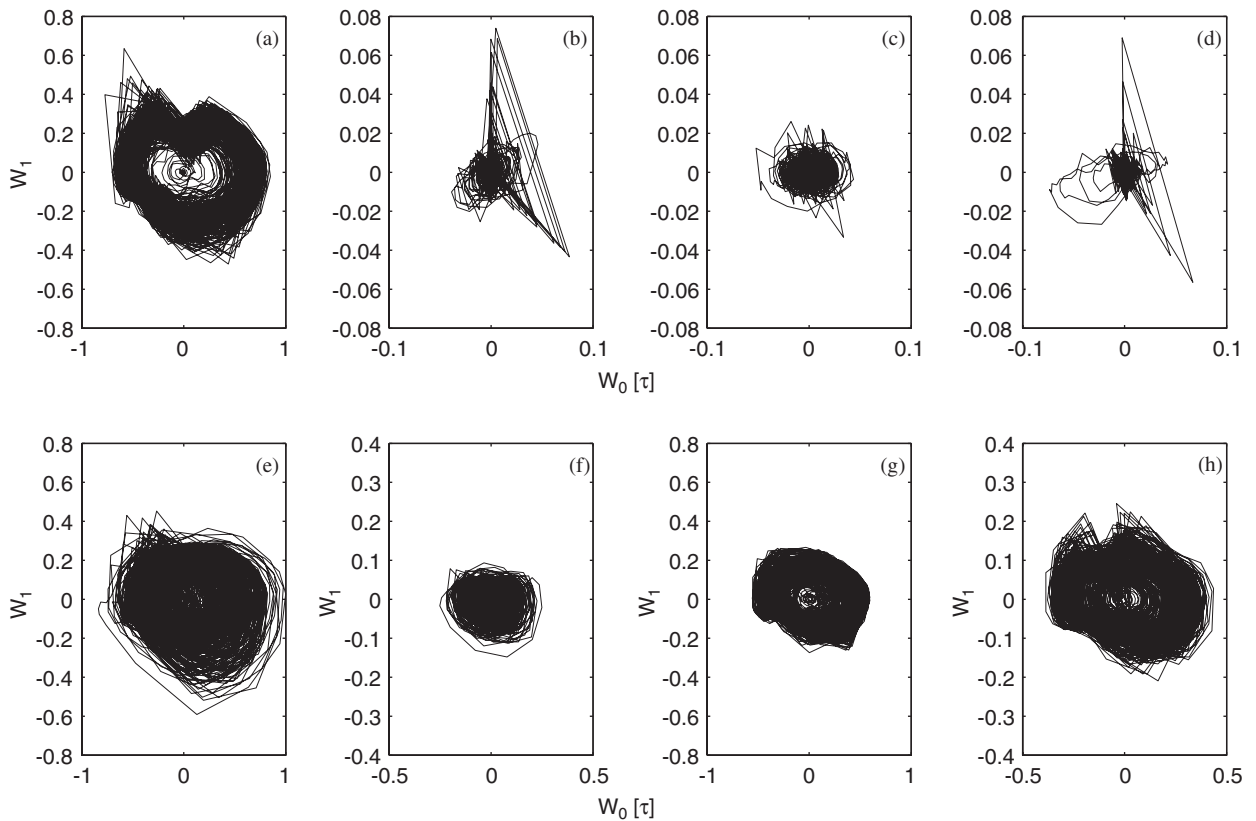
Fig. 3. The phase portraits of the two first orthogonal dynamic variables $\mathbf{W}_0, \mathbf{W}_1$ for pathological tremor in the patient with Parkinson's disease. The phase portraits are submitted according to the initial time series. The form of the phase portraits reflects the initial time signal dynamics. The periodic structure of the initial signal is determined by helicoidal phase trajectories (a, e–h); the randomness of the initial signal is reflected in the curvature of the phase trajectories (b–d). The most significant fluctuations of the time signal cause deformation of the phase portraits under any medical influence. The similar forms of phase clouds are characteristic of all the groups of patients.

shows that the higher value of $\varepsilon_1(0) \sim 10^1$ corresponds to the smaller pathological tremor velocity. For the smallest pathological tremor velocities (in one of the patients of the studied group) the values of this parameter are maximal and achieve the value of $\varepsilon_1(0) \sim 10^2$. On the contrary, the decrease of this parameter reflects the amplification of non-Markov effects in the initial time series. Thus, the decrease of parameter $\varepsilon_1(0)$ corresponds to the increase in Parkinsonian tremor velocity in the initial time signal. The greatest pathological tremor velocities (for one of the patients of the studied group) are characterized by minimal values $\varepsilon_1(0) \sim 10^0$. Thus, the value of $\varepsilon_1(0)$ reflects the behavior of the patient's tremor amplitude.

It should be noted that we use the value of the first point of the non-Markovity parameter at zero frequency $\varepsilon_1(0)$ as the quantitative measure which reflects Markov and non-Markov effects in the initial time series. The values of the non-Markovity parameter at zero frequency determine long-range correlations (in a limiting case for $t \to \infty$). The greater values of parameter $\varepsilon_1(0)$ determine stronger correlations. This thesis confirms a general concept that long-range correlations should take place in a stable healthy live subject. We remind that in this work we analyze the time series of pathological tremor of a patient and we observe only minimal alterations of parameter $\varepsilon_1(0)$ (from a unit up to several tens).

The periodic structure of pathological tremor velocity is reflected also in frequency dependences of the first point of the non-Markovity parameter (Figs. 5a, e–h). Oscillations emerge with a characteristic frequency $v \sim 5.2$ Hz. The oscillations are most appreciable in the low-frequency range. This structure is completely suppressed by medical influence on the patient's organism. The fast change of various dynamic modes and the amplification of randomness effects result in the infringement of the periodic picture. It is connected with the decrease of pathological tremor, the "ON–ON", "OFF–ON" states (Figs. 5b, d).
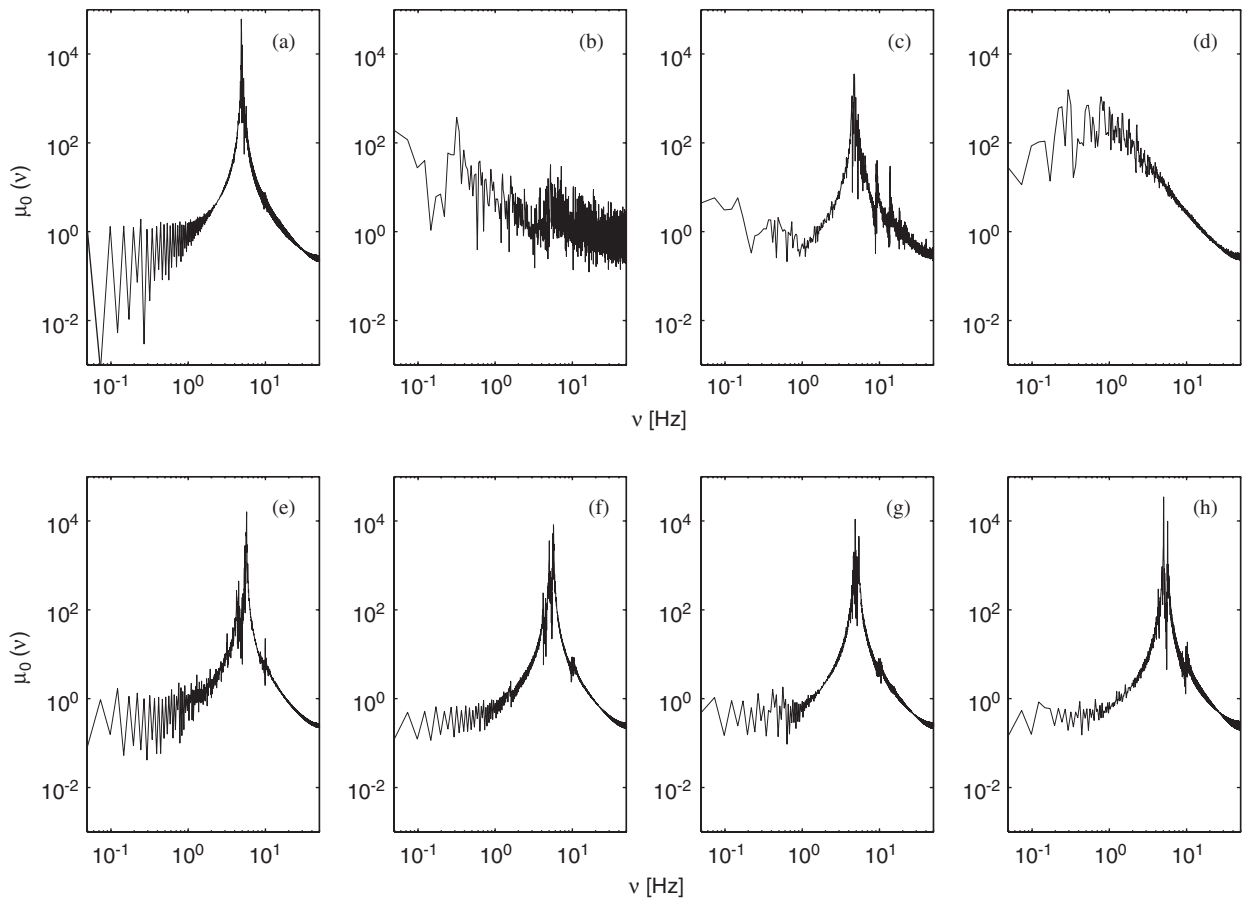
Fig. 4. The initial time correlation function $\mu_0(v)$ power spectrum for pathological tremor in the patient with Parkinson's disease. The power spectra are submitted according to the arrangement of the initial time series. The log–log scale is chosen to receive a more detailed information. In the initial TCF $\mu_0(v)$ power spectrum the power peak is observed on frequency $v = 5.2$ Hz. The amplitude of this peak is determined by the amplitude of the initial time signal. The oscillations (a, e–h) are clearly expressed in the low frequencies area of the power spectrum. The low-frequency oscillations vanish, and the amplitude of the power peak on frequency $v = 5.2$ Hz decreases with the application of any method of treatment (b–d). The amplitude of this peak changes a little bit when the DBS is used. It reflects low efficiency of this method of treatment (of the sixth patient). The form of power spectrum $\mu_0(v)$ is determined by the nature of the initial time signals.

The analysis of the values of parameter $\varepsilon_1(0)$ in different states of the patient specifies the most effective method of treatment (pathological tremor suppression). Values $\varepsilon_1(0)_M = 14.87$ in the "OFF–ON" patient's state (using medicaments) and $\varepsilon_1(0)_{ON} = 13.53$ in the "ON–ON" patient's state (using medicaments and the DBS) show, that these methods of treatment have almost the same positive effects. For comparison: we have $\varepsilon_1(0)_{DBS} = 3.56$ in the "ON–OFF" state of the studied patient (using the DBS), and $\varepsilon_1(0)_{OFF} = 1.47$ in the "OFF–OFF" state of the patient (no treatment).

The window-time behavior of the initial TCF power spectrum $\mu_0(v)$ (Fig. 6a) and the first point of the non-Markov parameter $\varepsilon_1(v)$ (Fig. 6b) is shown in Fig. 6. For example, we selected the initial time series in the "OFF–OFF" patient's state. The design of this dependence was realized by means of the localization procedure. The peculiarity of this procedure consist in reflecting the dynamical properties of the local area of the initial time signal [13]. First, the optimal length of the sample (window) must be determined. The preliminary analysis of various window lengths gave the optimal length of $256 = 2^8$ points. The correlation function power spectrum $\mu_0(v)$ and the non-Markovity parameter $\varepsilon_1(v)$ are calculated for each of the windows. This procedure shows the dynamic features of local areas of the initial time signal.
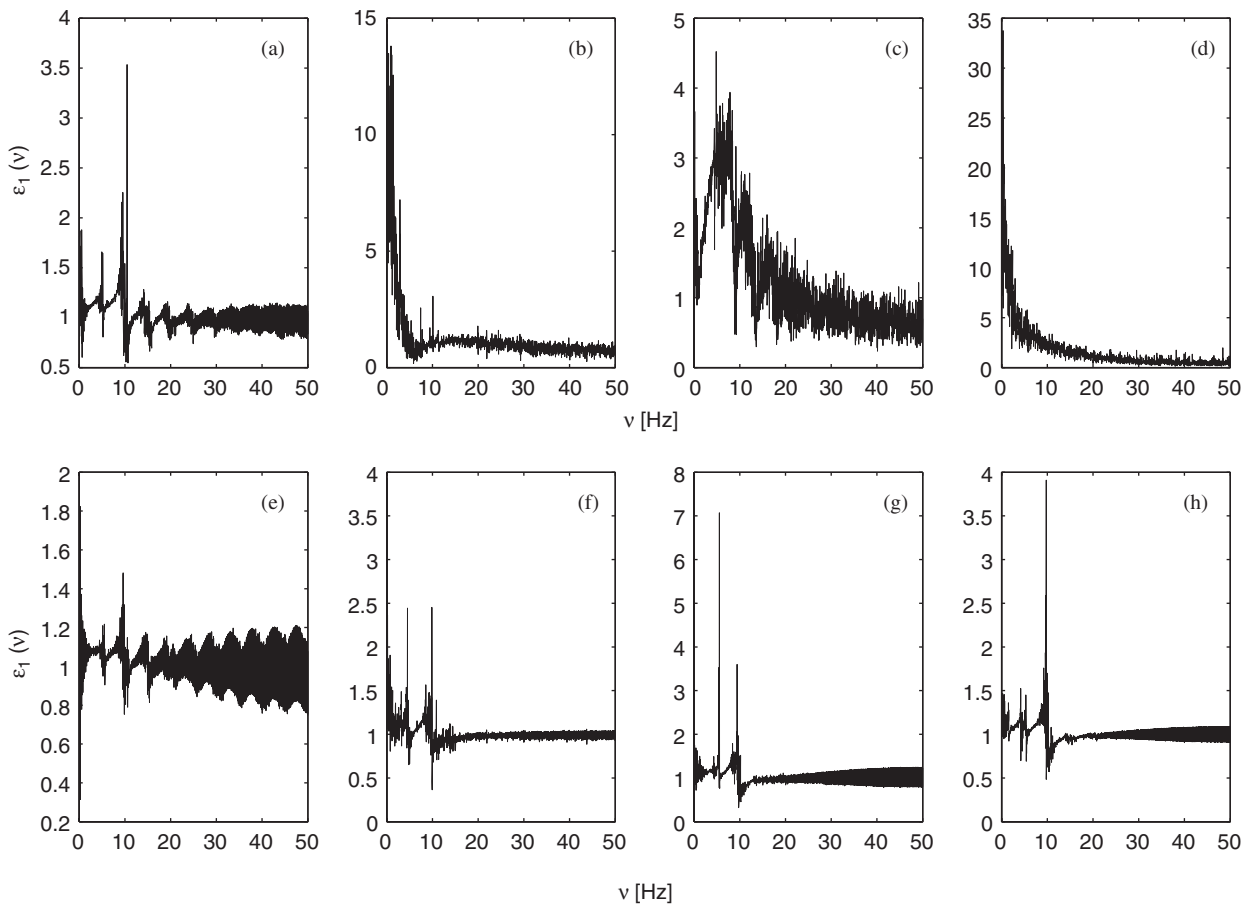
Fig. 5. The frequency dependence of the first point of the non-Markovity parameter $\varepsilon_1(\nu)$ for pathological tremor velocity in the patient. For example, the sixth patient with Parkinson's disease is chosen. The figures are submitted according to the arrangement of the initial time series. The characteristic low-frequency oscillations are observed in frequency dependences (a, e–h), which get suppressed under medical influence (b–d). The non-Markovity parameter reflects the Markov and non-Markov components of the initial time signal. The value of the parameter on zero frequency $\varepsilon_1(0)$ reflects the total dynamics of the initial time signal. The maximal values of parameter $\varepsilon_1(0)$ correspond to small amplitudes of pathological tremor velocity. The minimal values of this parameter are characteristic of significant pathological tremor velocities. The comparative analysis of frequency dependences $\varepsilon_1(\nu)$ allows us to estimate the efficiency of each method of treatment.

In Fig. 6a power peaks are observed at frequency $\nu = 5.2\,\mathrm{Hz}$ in the window-time behavior of the initial TCF power spectrum. The amplitude of these peaks reflects the increase or decrease in Parkinsonian tremor. In particular, the most significant peaks are visible for windows 1–3. Thus, the highest pathological tremor of the initial time record corresponds to these areas. The similar behavior of the power spectrum confirms the periodic nature of the initial time signal. The behavior of the non-Markovity parameter $\varepsilon_1(\nu)$ in Fig. 6b is as follows. The value of parameter $\varepsilon_1(0)$ reaches a unit (see, windows 1–3, 8, 11, 13) at the moments of the increase in pathological tremor velocity. Thus, the value of the non-Markovity parameter starts to decrease 2.5–3 s before the increase in tremor velocity. When pathological tremor velocity decreases, the value of parameter $\varepsilon_1(0)$ increases to values 2–3 (in the "OFF–OFF" patient's state, no treatment).

In Table 1 we present the root-mean-square amplitude $\langle A \rangle = \{\sum_{j=0}^{N-1} x_j^2/N\}^{1/2}$, and the dispersion $\sigma^2 = (1/N)\sum_{j=0}^{N-1}(x_j - \langle X \rangle)^2$ of kinetic parameter λ_1 for the sixth patient. The physical meaning of parameter λ_1 consists in determining the relaxation rate of the studied process [14]. The ratio of the mean-squared amplitude in the "OFF–OFF" patient's state (no treatment) and in the "ON–ON" patient's state (using medicaments
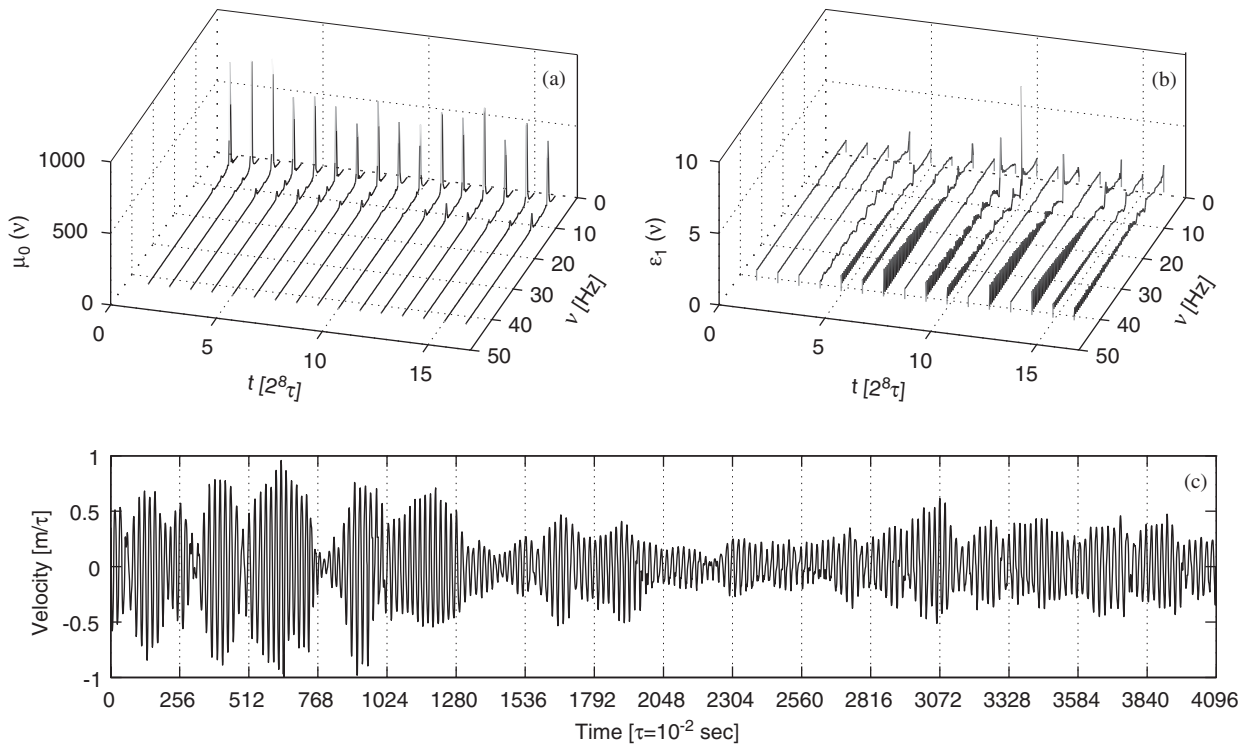
Fig. 6. The window-time behavior of the power spectrum $\mu_0(v)$ (a) and the frequency dependence of parameter $\varepsilon_1(v)$ (b) for pathological tremor in the "OFF–OFF" condition (c). The local representation of the TCF power spectrum and the frequency dependence of the non-Markovity parameter allows us to reflect the dynamic features of some areas of the time series. The localization procedure consists in choosing the optimum length of the local sample, in dividing the time series and in designing local characteristics for each sample. The increase of pathological tremor velocity results in the increase of the amplitude of the power peaks at a characteristic frequency and in the decrease of the non-Markovity parameter to a unit.

Table 1
The root-mean-square amplitude $\langle A \rangle$, and dispersion σ^2 (absolute values) of the first kinetic parameter λ_1 in various physiological states of the sixth patient, calculated by means of our theory

	OFF–OFF	ON–ON	ON–OFF	OFF–ON	15 OFF	30 OFF	45 OFF	60 OFF
$\langle A \rangle$	17.4×10^{-5}	43.4×10^{-3}	21.7×10^{-3}	52.4×10^{-3}	10.7×10^{-5}	10.6×10^{-5}	10.4×10^{-5}	13.8×10^{-5}
σ^2	59.3×10^{-3}	0.392	0.291	0.569	51.5×10^{-3}	62.2×10^{-3}	63.3×10^{-3}	61.3×10^{-3}

1—DBS, 2—Medication (L-Dopa). For example, OFF–OFF—DBS off, medication off.

and the DBS) makes 250 (!) times. It shows, that after the application of any type of treatment, relaxation rate increases. Sharp distinctions of relaxation rate reflect pathological and normal physiological processes. Thus, this quantitative characteristic allows to reveal effective or inefficient methods of treatment (to decrease tremor velocity).

5.2. The use of the flicker-noise spectroscopy for the analysis of pathological tremor velocity caused by Parkinson's disease

In Fig. 7 the power spectra of high-frequency $S_F(f)$ (Figs. 7a–d) and low-frequency $S_R(f)$ (Figs. 7e–h) components of the initial time signal (the tremor of the index finger velocity in the four patient's states, see Figs. 1a–d) are shown. Frequency dependence of the power spectrum of high-frequency component $S_F(f)$ is
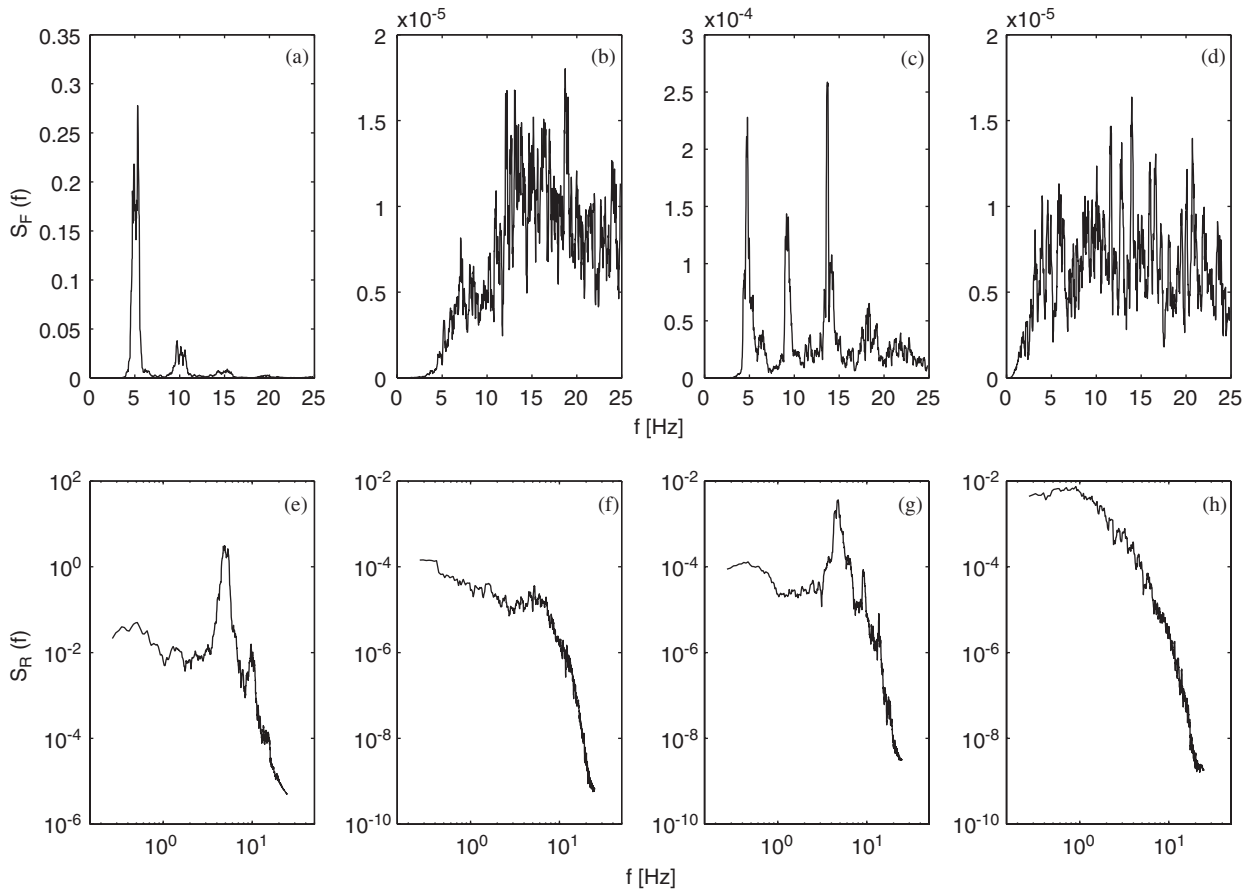
Fig. 7. The power spectra of high-frequency (a–d) and low-frequency (e–h) components of the initial time signal in the "OFF–OFF" condition (a, e) and in various conditions of treatment: medicaments and the DBS ("ON–ON" condition) (b, f), the DBS only ("ON–OFF" condition) (c, g), medicaments only ("OFF–ON" condition) (d, h). The power spectra of high-frequency component F are submitted on a linear scale (a–d), the power spectra of low-frequency component R are submitted on a log–log scale (e–h). The set of eigenfrequencies in the power spectra is connected to the periodic nature of Parkinsonian tremor.

on a linear scale, and the power spectrum of low-frequency component of time signal $S_R(f)$ is on a log–log scale. The small set of eigenfrequencies is characteristic of tremor of the "OFF–OFF" patient's state (Figs. 7a, e). These frequencies are clearly visible at $f_{01} \sim 5.2$ Hz and $f_{02} \sim 10.1$ Hz. According to Figs. 7c, g, the situation does not change qualitatively, when the DBS ("ON–OFF" patient's state) is used, as the small set of eigenfrequencies of tremor is preserved. However, the maximal values of $S_F(f)$ decrease by three orders and maximal values of $S_R(f)$ decrease by two orders. The situation changes qualitatively when medicaments are used ("OFF–ON", Figs. 7d, h), and also in case of the combined use of the DBS and medicaments ("ON–ON", Figs. 7b, f). Tremor velocity in these cases becomes more chaotic, since a wide band of eigenfrequencies appears in the tremor power spectrum. The maximal values of frequencies in dependence $S_F(f)$ decrease by four orders, the values of $S_R(f)$ decrease in the low frequencies range by two orders under the combined use of the DBS and medicaments ("ON–ON"). Values $S_R(f)$ in the low-frequencies area (when using medicaments, "OFF–ON") are commensurable with values $S_R(f)$ in the "OFF–OFF" state.

The specific features characterizing tremor velocity in the patient with PD are seen in spectra $S_F(f)$ and $S_R(f)$ in Figs. 7a–h. It should be noted that the splitting of the initial time signal $x(t)$ into components $x_R(t)$ and $x_F(t)$ depends on quantity N of iterations of "diffusion" smoothing and the value of "diffusion coefficient" D ($N = 10$ and $D = \frac{1}{4}$ for the plots). The analysis shows that the increase of the number of such
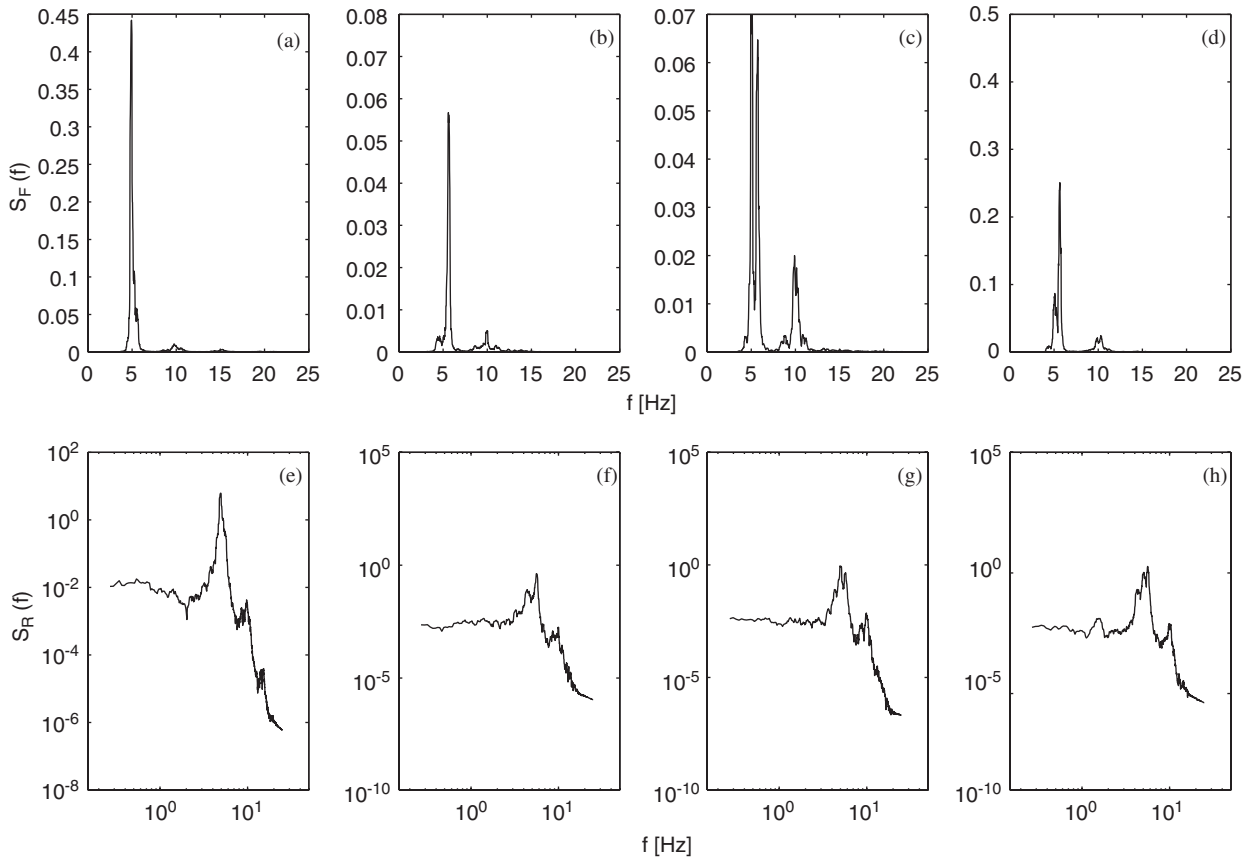
Fig. 8. The power spectra of high-frequency (a–d) and low-frequency (e–h) components of Parkinsonian tremor velocity in the patient's states 15 (a, e), 30 (b, f), 45 (c, g), 60 (d, h) min after the DBS is switched off. The high-frequency component F is submitted on a linear scale, the low-frequency R is submitted on a log–log scale. From these figures it is visible, that by switching off the DBS we get the insignificant decrease of the resonant component of the initial signal.

iterations up to $N = 50$ for various values of parameter D does not change the obtained results essentially. Therefore, we use values $N = 10$ and $D = 1/4$ to calculate FNS dependences in the following way.

Fig. 8 shows the dynamics of tremor velocity of the patient in the cases when the DBS is switched off. The use of this medical methods does not change the situation. The small set of eigenfrequencies of tremor velocity remains the same. However, there is significant decrease in the maximal values of power spectra $S_F(f)$ and $S_R(f)$. Frequency dependence $S_F(f)$ should be considered as information valuable patterns when determining the characteristic frequencies of the system, as $S_R(f)$ dependence do not changes significantly (see Fig. 8).

The difference moments of low- and high-frequency components of the initial signal $\Phi_R^{(2)}(\tau)$, $\Phi_F^{(2)}(\tau)$ can also carry valuable information about tremor dynamics. It is seen in Figs. 9 and 10. This dependence characterizes the duration of correlation interval T_1 during which "a loss of memory" about the local value of the signal takes place.

The combined use of the DBS and medicaments ("ON–ON", Figs. 9b, f) results in the strongest changes in tremor velocity: the dispersion of fluctuations decreases by two orders and the contribution of "resonance" frequencies is considerably suppressed. It is seen in Fig. 9. The latter conclusion follows from the decrease of the oscillatory component.

Time dependence in Fig. 10 characterizes the dynamics of pathological tremor velocity in the patient's states when the DBS is switched off ("15 OFF", "30 OFF", "45 OFF", "60 OFF"). The comparative analysis of Figs. 9 and 10 shows that the initial parameters of the patient's tremor ("OFF–OFF" state) almost do not vary. Thus, the dispersion of fluctuations somewhat decreases and the "resonance" component of the initial signal actually does not change.
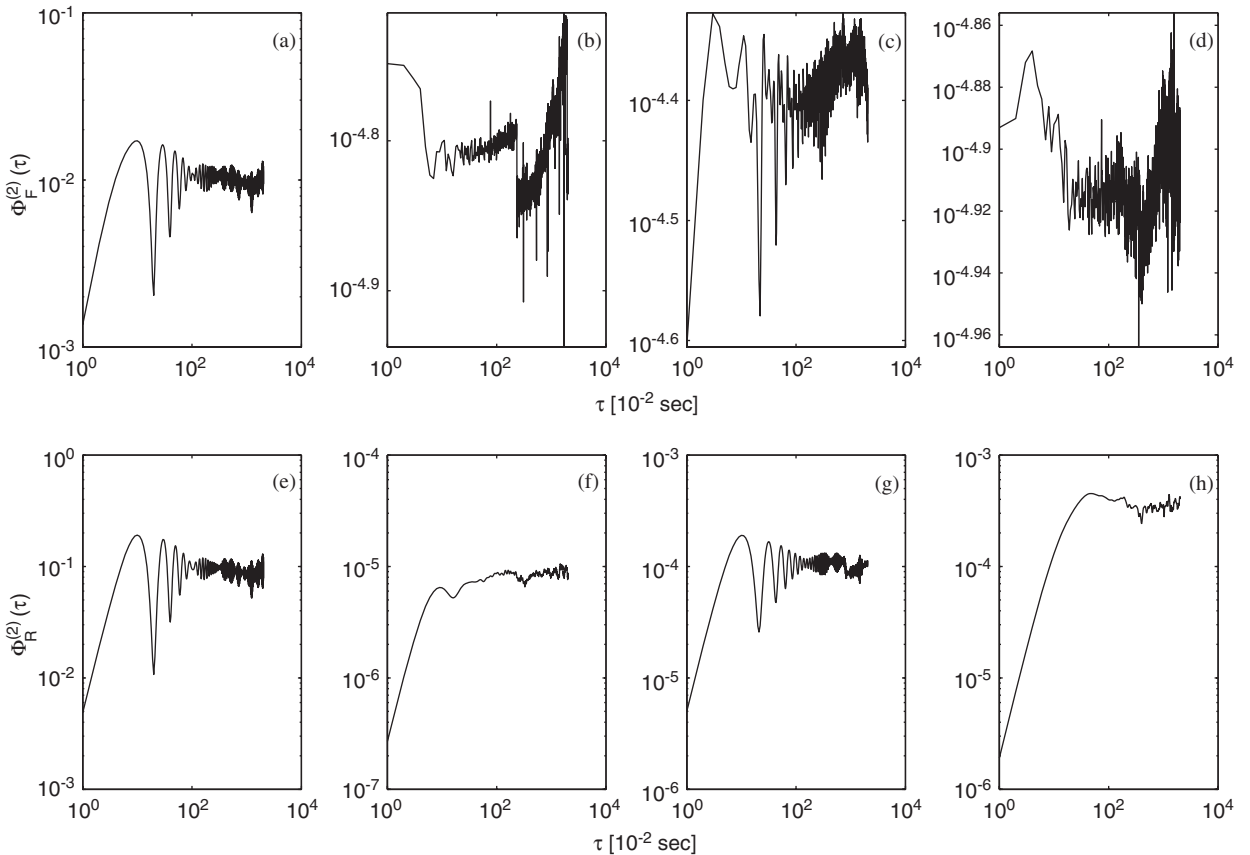
Fig. 9. The difference moments of the second order for high-frequency component F and low-frequency component R in the states of the patient: (a, e) no treatment ("OFF–OFF" condition); (b, f) complex treatment ("ON–ON" condition); (c, g) the DBS only ("ON–OFF" condition); (d, h) medicaments only ("OFF–ON" condition). The figures are submitted on a log–log scale. The behavior of difference moments $\Phi_F^{(2)}(\tau)$, $\Phi_R^{(2)}(\tau)$ becomes more stochastic in any case of medical influence.

6. Conclusions. The analysis of pathological tremor caused by Parkinson's disease

In this work we offer a new method of analyzing one of the symptoms of PD. This method is based on the combined use of the statistical theory of discrete non-Markov stochastic processes and the FNS. Each of the offered theories reflects the specific dynamic peculiarities of PD tremor. Combined representation of the obtained results allows to extract the most complete and trustworthy information about the dynamics of Parkinsonian tremor.

As experimental data we used the time series of the tremor velocity of an index finger of the patient with PD for various methods of treatment. The tremor of a human's limbs certainly is just one of the external symptoms of PD. However, the tremor dynamics of a human's limb is caused by complex interrelation of separate areas of brain, central nervous system, locomotor system, chemical and biological metabolism. Any anomaly of one of these systems is clearly reflected in tremor dynamics. The analysis of the stochastic dynamics of a human's index finger tremor is only part of the complex analysis of the patient's states.

The analysis of stochastic dynamics of the pathological tremor velocity shows the change of the physical nature of the signal. The robust periodic structure with specific oscillation frequency is characteristic of the time series of pathological tremor velocity in "OFF–OFF" patient's state (no treatment). The similar structure of the initial time signal is connected to the pathological tremor of the limbs in the patient with PD. The structure of the signal changes and becomes more stochastic when the patient undergoes treatment. The
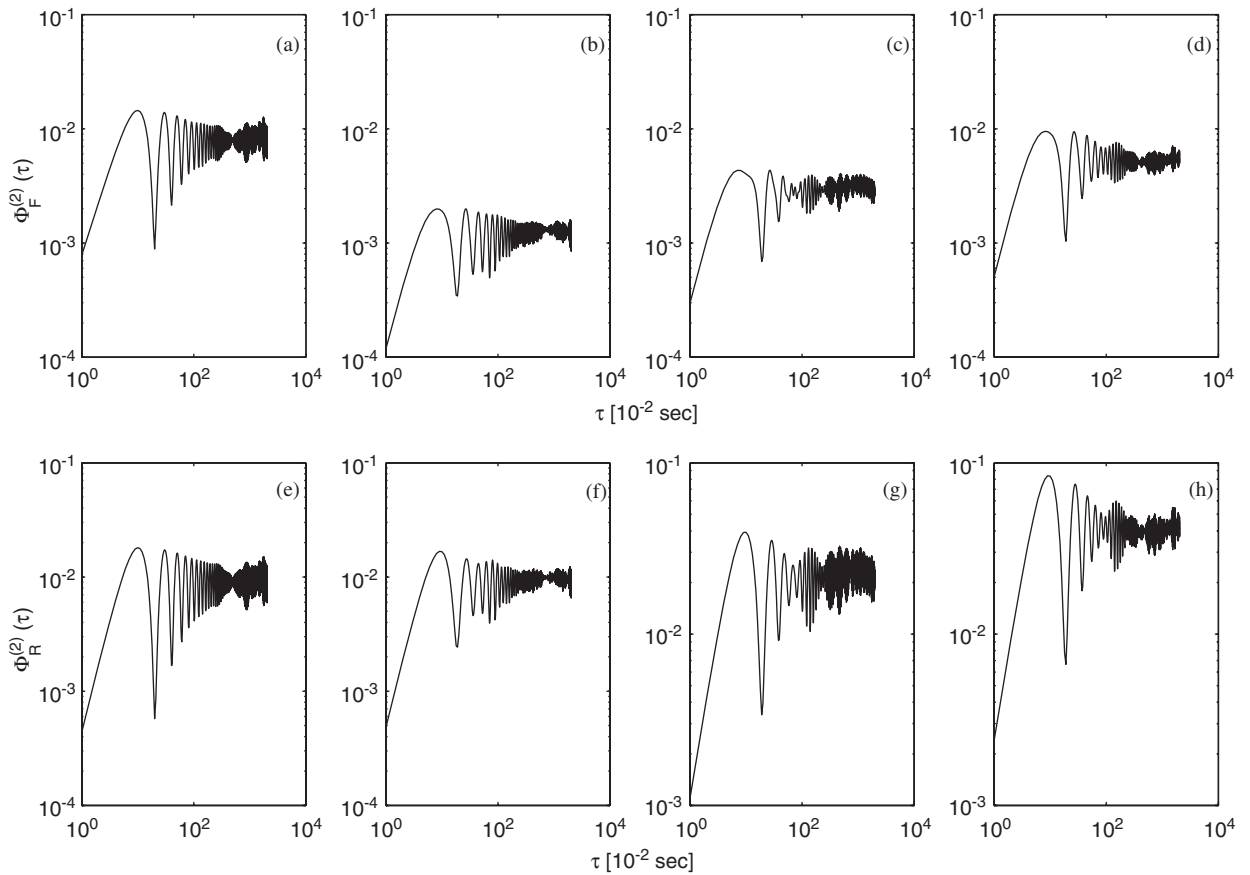
Fig. 10. The difference moments of the second order for high-frequency component F and low-frequency component R of Parkinsonian tremor in the patient: (a, e) 15 min after the DBS is switched off; (b, f) 30 min after the DBS is switched off; (c, g) 45 min after the DBS is switched off; (d, h) 60 min after the DBS is switched off. Medicaments are not used. The figures are submitted on a log–log scale. The aftereffects of the DBS render insignificant influence on the initial characteristics of tremor velocity.

amplification of stochastic effects in the initial signal is connected to the increase of degrees of freedom in the studied system. Their maximal value corresponds to a normal physiological state.

The first technique consists in determining the Markov and non-Markov components of the initial time signal, manifestation of long- and short-range statistical memory effects, the amplification and degradation of correlations in the initial time signal. This technique also allows to reveal the effects of randomness, regularity and periodicity, dynamic alternation effects of various relaxation processes for overall initial time series and their local areas. The statistical theory of discrete stochastic non-Markov processes makes it possible to obtain the whole spectrum of quantitative and qualitative values and the characteristics based on the information carried by fluctuations and correlations in the initial time signals.

The stochastic dynamics of pathological tremor velocity in various dynamic states of a patient with PD is clearly reflected in the phase portraits of orthogonal variables, in power spectra of a correlation function and memory functions of the lower orders, in frequency dependences of the non-Markov parameter, in local relaxation and kinetic parameters. The analysis of all the information about the correlations and fluctuations of the initial time series allows to estimate the efficiency of different methods of treatment. For example, we analyzed the experimental data of one of the patients with PD.

We used the statistical spectrum of the non-Markovity parameter to reveal Markov and non-Markov effects in the initial time series. The increase or decrease of pathological tremor velocity predetermines the changes of the statistical non-Markovity parameter. The increase of the stochastic effects and the Markov components of the initial time signal and the manifestation of long-range correlations correspond to the decrease of

pathological tremor velocity. At the same time the increase of pathological tremor velocity is accompanied by the occurrence of the effects of periodicity and regularity, harmonic oscillations, non-Markov effects, the manifestation of memory effects and degradation of correlations in the initial time signals.

The described localization procedure reflects the dynamic properties of pathological tremor in some local areas of the initial time series. The window-time behavior of the initial TCF $\mu_0(v)$ and the first point of the non-Markovity parameter $\varepsilon_1(v)$ reflects the predictors of changes in pathological tremor velocity. Any changes of pathological tremor are instantly reflected in the window-time behavior of the dynamic characteristics.

Dynamic characteristics $\langle A \rangle$ and σ^2 of relaxation parameter λ_1 reflect relaxation rate in various dynamic patient's states. The use of any method of treatment results in acceleration of stabilization process. Significant distinctions in the dynamic characteristics of parameter λ_1 in the state of the patient with no treatment ("OFF–OFF" condition) and in the complex use of medicaments and the DBS ("ON–ON" condition) allow to estimate the relaxation scales of physiological processes for healthy and sick people.

Finally, the change of the nature of the pathological tremor time signal results in the change of the whole set of quantitative and qualitative characteristics and exponents. The general algorithm of these changes can be determined in the following way. The structure of the initial time series becomes more stochastic with reduction of Parkinsonian tremor velocity. The increase of the number of degrees of freedom determines predominance of Markov effects, manifestation of long-range correlations and more significant velocity of relaxation processes. The regularization of the initial time signal is observed with the increase of pathological tremor velocity (when this or that treatment is stopped), i.e., its structure becomes more robust. This fact is reflected in the behavior of the physical characteristics. The structure of phase clouds changes, the height of the peak on the characteristic frequency in the initial TCF power spectra increases, characteristic oscillations in the frequency spectra of the non-Markovity parameter appear, the value of the first point of the non-Markovity parameter on zero frequency decreases to 1.

The use of the FNS confirms the conclusion about the resonant character of the amplitude of Parkinsonian tremor velocity. It is necessary to note that the influence of the resonant tremor component decreases, and the stochastic tremor component increases under treatment. At the same time the analysis of spectral dependences and different moments of the second order, as well as the splitting of the signal into "high-frequency" and "low-frequency" components have allowed to make the timely estimate of the patient's state (Figs. 8 and 10) and the efficiency of different methods of treatment (Figs. 7 and 9). The estimates, which we have received, can be used to choose the "treatment strategy" for the patient. It is necessary to note, that the high-frequency component of pathological tremor velocity $S_F(f)$ is most sensitive to the changes arising in the initial time signal. On the whole, the method of the FNS allows to reveal the set of the eigenfrequencies and the resonant or the stochastic components of the initial time signal in various physiological states of the patient. This method elicits additional information about the effects of dynamic alternation and the nonstationary effects in the initial time series.

The methods of the time series analysis which are submitted in this paper, give a simple quantitative method or a graphic scheme for the analysis of various physiological states of a patient with PD. Each of these methods is independent and reflects unique local information about the initial time signal structure.

The obtained results allow us to use the offered methods for the analysis of other complex systems of biological nature. In particular, the offered methods have already made it possible to receive significant results in the statistical analysis of the experimental data of epidemiology, cardiology, neurophysiology and of human locomotion.

References

[1] R. Yulmetyev, P. Hänggi, F. Gafarov, Stochastic dynamics of time correlation in complex systems with discrete current time, Phys. Rev. E 62 (2000) 6178–6194.

[2] R. Yulmetyev, P. Hänggi, F. Gafarov, Quantification of heart rate variability by discrete nonstationary non-Markov stochastic processes, Phys. Rev. E 65 (2002) 046107-1-15.

[3] I. Goychuk, P. Hänggi, Stochastic resonance in ion channels characterized by information theory, Phys. Rev. E 61 (4) (2000) 4272–4280.

[4] I. Goychuk, P. Hänggi, Non-Markovian stochastic resonance, Phys. Rev. Lett. 91 (2003) 070601-1-4.

[5] I. Goychuk, P. Hänggi, Theory of non-Markovian stochastic resonance, Phys. Rev. E 69 (2004) 021104-1-15.

[6] L. Gammaitoni, P. Hänggi, P. Jung, F. Marchesoni, Stochastic resonance, Rev. Mod. Phys. 70 (1998) 223–288.

[7] R. Yulmetyev, A. Mokshin, P. Hänggi, Diffusion time-scale invariance, randomization processes, and memory effects in Lennard–Jones liquids, Phys. Rev. E 68 (2003) 051201-1-5.

[8] R. Yulmetyev, A. Mokshin, M. Scopigno, P. Hänggi, New evidence for the idea of timescale invariance of relaxation processes in simple liquids: the case of molten sodium, J. Phys.: Condens. Matter 15 (2003) 2235–2257.

[9] A.V. Mokshin, R.M. Yulmetyev, P. Hänggi, Diffusion processes and memory effects, New J. Phys. 7 (2005) 9-1-10.

[10] R. Yulmetyev, F. Gafarov, P. Hänggi, R. Nigmatullin, S. Kayumov, Possibility between earthquake and explosion seismogram differentiation by discrete stochastic non-Markov processes and local Hurst exponent analysis, Phys. Rev. E 64 (2001) 066132-1-14.

[11] R.M. Yulmetyev, A.V. Mokshin, P. Hänggi, Universal approach to overcoming nonstationarity, unsteadiness and non-Markovity of stochastic processes in complex systems, Physica A 345 (2005) 303–325.

[12] R.M. Yulmetyev, S.A. Demin, N.A. Emelyanova, F.M. Gafarov, P. Hänggi, Stratification of the phase clouds and statistical effects of the non-Markovity in chaotic time series of human gait for healthy people and Parkinson patients, Physica A 319 (2003) 432–446.

[13] R.M. Yulmetyev, P. Hänggi, F.M. Gafarov, Stochastic processes of demarkovization and markovization in chaotic signals of the human brain electric activity from EEGs at epilepsy, JETP 123 (3) (2003) 643–652.

[14] R.M. Yulmetyev, N.A. Emelyanova, S.A. Demin, F.M. Gafarov, P. Hänggi, D.G. Yulmetyeva, Non-Markov stochastic dynamics of real epidemic process of respiratory infections, Physica A 331 (2004) 300–318.

[15] V.V. Smolyaninov, Spatio-temporal problems of locomotion control, Phys. Usp. 170 (10) (2000) 1063–1128.

[16] D.A. Winter, Biomechanics of normal and pathological gait: implications for understanding human locomotion control, J. Motor. Behav. 21 (1989) 337–355.

[17] K.G. Holt, S.F. Jeng, R. Ratcliffe, J. Hamill, Energetic cost and stability during human walking at the preferred stride frequency, J. Motor. Behav. 27 (2) (1995) 164–178.

[18] J.B. Dingwell, J.P. Cusumano, Nonlinear time series analysis of normal and pathological human walking, Chaos 10 (4) (2000) 848–863.

[19] J. Timmer, M. Lauk, W. Pfleger, G. Deuschl, Cross-spectral analysis of physiological tremor and muscle activity. I Theory and application to unsynchronized electromyogram, Biol. Cybern. 78 (1998) 349–357.

[20] J. Timmer, M. Lauk, W. Pfleger, G. Deuschl, Cross-spectral analysis of physiological tremor and muscle activity. II Application to synchronized electromyogram, Biol. Cybern. 78 (1998) 359–368.

[21] J. Timmer, Modeling noisy time series: Physiological tremor, Chaos Appl. Sci. Eng. 8 (1998) 1505–1516.

[22] J. Timmer, S. Häußler, M. Lauk, C.H. Lücking, Pathological tremors: deterministic chaos or nonlinear stochastic oscillators?, Chaos 10 (1) (2000) 278–288.

[23] N. Sapir, R. Karasik, S. Havlin, E. Simon, J.M. Hausdorff, Detecting scaling in the period dynamics of multimodal signals: application to Parkinsonian tremor, Phys. Rev. E 67 (2003) 031903-1-8.

[24] B.J. West, N. Scafetta, Nonlinear dynamical model of human gait, Phys. Rev. E 67 (2003) 051917-1-10.

[25] J.M. Hausdorff, D.E. Forman, Z. Ladin, D.R. Rigney, A.L. Goldberger, J.Y. Wei, Increased walking variability in elderly persons with congestive heart failure, J. Am. Geriatr. Soc. 42 (1994) 1056–1061.

[26] J.M. Hausdorff, C.K. Peng, Z. Ladin, J.Y. Wei, A.L. Goldberger, Fractal dynamics of human gait: stability of long-range correlations in stride interval fluctuations, J. Appl. Physiol. 80 (1996) 1148–1457.

[27] J.M. Hausdorff, H.K. Edelberg, S.L. Mitchell, A.L. Goldberger, J.Y. Wei, Increased gait unsteadiness in community-dwelling elderly fallers, Arch. Phys. Med. Rehabil. 78 (1997) 278–283.

[28] J.M. Hausdorff, L. Zemany, C.K. Peng, A.L. Goldberger, Maturation of gait dynamics: stride-to-stride variability and its temporal organization in children, J. Appl. Physiol. 86 (1999) 1040–1047.

[29] J.M. Hausdorff, S.L. Mitchell, R. Firtion, C.K. Peng, M.E. Cudkowicz, J.Y. Wei, A.L. Goldberger, Altered fractal dynamics of gait: reduced stride interval correlations with aging and Huntington's disease, J. Appl. Physiol. 82 (1997) 262–269.

[30] J.M. Hausdorff, M.E. Cudkowicz, R. Firtion, H.K. Edelberg, J.Y. Wei, A.L. Goldberger, Gait variability and basal ganglia disorders: stride-to-stride variations in gait cycle timing in Parkinson's and Huntington's disease, Mov. Disord. 13 (1998) 428–437.

[31] A. Beuter, R. Edwards, Using frequency domain characteristics to discriminate physiologic and parkinsonian tremors, J. Clin. Neurophys. 16 (5) (1999) 484–494.

[32] R. Edwards, A. Beuter, Using time domain characteristics to discriminate physiologic and parkinsonian tremors, J. Clin. Neurophys. 17 (1) (2000) 87–100.

[33] A. Beuter, R. Edwards, Kinetic tremor during tracking movements in patients with Parkinson's disease, Parkinsonism Relat. Disord. 8 (2002) 361–368.

[34] D.E. Vaillancourt, K.M. Newell, Amplitude modulation of the 8–12 Hz, 20–25 Hz, and 40 Hz oscillations in finger tremor, J. Clin. Neurophys. 111 (2000) 1792–1801.

[35] D.E. Vaillancourt, A.B. Slifkin, K.M. Newell, Regularity of force tremor in Parkinson's disease, J. Clin. Neurophys. 112 (2001) 1594–1603.

[36] P. Maurer, H.-D. Wang, A. Babloyantz, Time structure of chaotic attractors: a graphical view, Phys. Rev. E 56 (1997) 1188–1196.

[37] A. Babloyantz, A. Destexhe, Is the normal heart a periodic oscillator?, Biol. Cybern. 58 (1988) 203–211.

[38] A. Goldbeter, Biochemical Oscillations and Cellular Rhythms: The Molecular Bases of Periodic and Chaotic Behaviour, Cambridge University Press, Cambridge, 1996.

[39] A. Goldbeter, D. Gonze, G. Houart, J.-C. Leloup, J. Halloy, G. Dupont, From simple to complex oscillatory behavior in metabolic and genetic control networks, Chaos 11 (1) (2001) 247–260.

[40] D. Gonze, J. Halloy, A. Goldbeter, Emergence of coherent oscillations in stochastic models for circadian rhythms, Physica A 342 (2004) 221–223.

[41] L.S. Liebovitch, M. Zóchowski, Dynamics of neural networks relevant to properties of proteins, Phys. Rev. E 56 (1997) 931–935.

[42] M. Zóchowski, L.S. Liebovitch, Synchronization of the trajectory as a way to control the dynamics of a coupled system, Phys. Rev. E 56 (1997) 3701–3704.

[43] M. Zóchowski, L.S. Liebovitch, Self-organizing dynamics of coupled map systems, Phys. Rev. E 59 (1999) 2830–2837.

[44] L.S. Liebovitch, W. Yang, Transition from persistent to antipersistent correlation in biological systems, Phys. Rev. E 56 (1997) 4557–4566.

[45] L.S. Liebovitch, A.T. Todorov, M. Zóchowski, D. Scheurle, L. Colgin, M.A. Wood, K.A. Ellenbogen, J.M. Herre, R.C. Bernstein, Nonlinear properties of cardiac rhythm abnormalities, Phys. Rev. E 59 (1999) 3312–3319.

[46] S.B. Lowen, L.S. Liebovitch, J.A. White, Fractal ion-channel behavior generates fractal firing patterns in neuronal models, Phys. Rev. E 59 (1999) 5970–5980.

[47] C.K. Peng, S.V. Buldyrev, A.L. Goldberger, S. Havlin, M. Simons, H.E. Stanley, Finite size effects on long-range correlations: implications for analyzing DNA sequences, Phys. Rev. E 47 (1993) 3730–3733.

[48] C.K. Peng, S. Havlin, H.E. Stanley, A.L. Goldberger, Quantification of scaling exponents and crossover phenomena in nonstationary heartbeat time series, Chaos 6 (1995) 82–87.

[49] R. Zwanzig, Ensemble method in the theory of irreversibility, J. Chem. Phys. 3 (1960) 106–141.

[50] R. Zwanzig, Memory effects in irreversible thermodynamics, Phys. Rev. 124 (1961) 983–992.

[51] H. Mori, Transport, collective motion and brownian motion, Prog. Theor. Phys. 33 (1965) 423–455.

[52] H. Mori, A continued fraction representation of the time correlation functions, Prog. Theor. Phys. 34 (1965) 399–416.

[53] S.F. Timashev, Complexity and evolutionary law for natural systems, in: C. Rossi, S. Bastianoni, A. Donati, N. Marchettini (Eds.), Tempos in Science and Nature: Structures, Relations, and Complexity, Annals of the New York Academy of Science, vol. 879, The New York Academy of Science, 1999, pp. 129–143.

[54] S.F. Timashev, Science of complexity: phenomenological basis and possibility of application to problems of chemical engineering, Theor. Found. Chem. Eng. 34 (2000) 301–312.

[55] S.F. Timashev, Flicker-noise spectroscopy as a tool for analysis of fluctuations in physical systems, in: G. Bosman (Ed.), Noise in Physical Systems and 1/f Fluctuations—ICNF 2001, World Scientific, New Jersey, London, 2001, pp. 775–778.

[56] S.F. Timashev, Flicker-noise spectroscopy in analysis of chaotic fluxes in distributed dynamical dissipative systems, Russ. J. Phys. Chem. 75 (10) (2001) 1742–1749.

[57] S.F. Timashev, G.V. Vstovskii, Flicker-noise spectroscopy of analyzing chaotic time series of dynamic variables: Problem of signal-to-noise relation, Russ. J. Electrochem. 39 (2) (2003) 141–153.

[58] G.V. Vstovsky, A.V. Descherevsky, A.A. Lukk, A.Ya. Sidorin, S.F. Timashev, Search for electric earthquake precursors by the method of flicker-noise spectroscopy, Izv. Phys. Solid Earth 41 (7) (2005) 513–524.

[59] S.F. Timashev, V.V. Grigor'ev, E.Yu. Budnikov, Flicker-noise spectroscopy in analysis of fluctuation dynamics of electric potential in electromembrane system under "overlimiting" current density, Russ. J. Phys. Chem. 76 (3) (2002) 475–482.

[60] V. Parkhutik, S.F. Timashev, Informative essence of noise: New finding in the electrochemistry of silicon, Russ. J. Electrochem. 36 (11) (2000) 1221–1235.

[61] V. Parkhutik, E. Rayon, C. Ferrer, S. Timashev, G. Vstovsky, Forecasting of electrical breakdown in porous silicon using flicker-noise spectroscopy, Phys. Status Solidi (A) 197 (2) (2003) 471–475.

[62] A.V. Descherevsky, A.A. Lukk, A.Ya. Sidorin, G.V. Vstovsky, S.F. Timashev, Flicker-noise spectroscopy in earthquake prediction research, NHESS 3 (3/4) (2003) 159–164.

[63] L. Telesca, V. Lapenna, S. Timashev, G. Vstovsky, G. Martinelli, Flicker-noise spectroscopy as a new approach to investigate the time dynamics of geoelectric signals measures in seismic areas, Phys. Chem. Earth, Parts A/B/C 29 (4–9) (2004) 389–395.

[64] V. Parkhutik, B. Collins, M. Sailor, G. Vstovsky, S. Timashev, Analysis of morphology of porous silicon layers using flicker-noise spectroscopy, Phys. Status Solidi (A) 197 (1) (2003) 88–92.

[65] S.F. Timashev, A.B. Solovieva, G.V. Vstovsky, Informative "passport data" of surface nano- and microstructures, in: J. Sikula, M. Levinshtein (Eds.), Advanced Experimental Method for Noise Research in Nanoscale Electronic Devices, Kluwer Academic Publisher, The Netherlands, 2004, pp. 177–186.

[66] I.G. Kostuchenko, S.F. Timashev, The comparative analysis of dynamic characteristics of solar-terrestrial processes, in: V.G. Gurzadyan, R. Ruffini (Eds.), Advanced Series in Astrophysics and Cosmology, The Chaotic Universe: Proceedings of the Second ICRA Network Workshop, vol. 10, Singapore, World Scientific, River Edge, NJ, 2000, pp. 579–589.

[67] S.F. Timashev, G.V. Vstovsky, A.B. Solovieva, Informative essence of chaos, in: L. Reggiani, C. Penneta, V. Akimov, E. Alfinito, M. Rosini (Eds.), Unsolved Problems of Noise and Fluctuations in Physics, Biology and High Technology, vol. 800, AIP Conference Proceedings, Melville, New York, 2005, pp. 368–374.

[68] S.F. Timashev, G.V. Vstovsky, A.Ya. Kaplan, A.B. Solovieva, What information is hidden in chaotic signals of biological systems? in: T. Gonzalez, J. Mateos, D. Pardo (Eds.), Noise and Fluctuations—ICNF-2005, AIP Conference Proceedings, vol. 780, Melville, New York, 2005, pp. 579–582.

[69] S.F. Timashev, Generalization of the fluctuation-dissipation relations, Russ. J. Phys. Chem. 79 (11) (2005) 1720–1727.

[70] H.G. Schuster, Deterministic Chaos. An Introduction, Physik-Verlag, Weinheim, 1984.

[71] A. Beuter, M.S. Titcombe, F. Richer, Ch. Gross, D. Guehl, Effects of deep brain stimulation on amplitude and frequency characteristics of rest tremor in Parkinson's disease, Thalamus Relat. Syst. 1 (2001) 203–211.

[72] M.S. Titcombe, L. Glass, D. Guehl, A. Beuter, Dynamics of Parkinsonian tremor during deep brain stimulation, Chaos 11 (4) (2001) 766–773.

[73] A. Beuter, A. de Geoffroy, P. Cordo, The measurement of tremor using simple laser systems, J. Neurosci. Meth. 53 (1994) 47–54.

[74] K.E. Norman, R. Edwards, A. Beuter, The measurement of tremor using a velocity transducer: comparison to simultaneous recordings using transducers of displacement, acceleration and muscle activity, J. Neurosci. Meth. 92 (1999) 41–54.